

EMERGENT MIXTURE-OF-EXPERTS: CAN DENSE PRE-TRAINED TRANSFORMERS BENEFIT FROM EMERGENT MODULAR STRUCTURES?

Zihan Qiu^{1*†}, Zeyu Huang^{2*}, Jie Fu^{3‡}

¹ IIIS, Tsinghua University

² ILCC, University of Edinburgh

³ CSE, The Hong Kong University of Science and Technology

qzh11628@gmail.com, zeyu.huang@ed.ac.uk, jiefu@ust.hk

ABSTRACT

Incorporating modular designs into neural networks demonstrates superior out-of-generalization, learning efficiency, etc. Existing modular neural networks are generally *explicit* because their modular architectures are pre-defined, and individual modules are expected to implement distinct functions. Conversely, recent works reveal that there exist *implicit* modular structures in standard pre-trained transformers, namely *Emergent Modularity*. They indicate that such modular structures exhibit during the early pre-training phase and are totally spontaneous. However, most transformers are still treated as monolithic models with their modular natures underutilized. Therefore, given the excellent properties of explicit modular architecture, we explore *whether and how dense pre-trained transformers can benefit from emergent modular structures*. To study this question, we construct **Emergent Mixture-of-Experts** (EMoE). Without introducing additional parameters, EMoE can be seen as the modular counterpart of the original model and can be effortlessly incorporated into downstream tuning. Extensive experiments (we tune 1785 models) on various downstream tasks (vision and language) and models (22M to 1.5B) demonstrate that EMoE effectively boosts in-domain and out-of-domain generalization abilities. Further analysis and ablation study suggest that EMoE mitigates negative knowledge transfer and is robust to various configurations. Code is available at <https://github.com/qiuzh20/EMoE>

1 INTRODUCTION

Modularity attracts considerable attention from the artificial intelligence community (Auda & Kamel, 1999). Neural networks with modular designs, termed Modular Neural Networks (MNN), have exhibited a wide range of advantages, including adaptation (Shen et al., 2023b), out-of-distribution (OOD) generalization abilities (Goyal & Bengio, 2020; Weiss et al., 2022), and data efficiency (Bengio et al., 2020). Typical MNNs are usually *explicitly* modular. Their modular structure is pre-defined and they are expected to achieve a divide-and-conquer solution for the given task. For example, Andreas et al. (2016) design separate visual and language functional modules and jointly train them to solve visual question-answering tasks. Among various MNNs, Mixture-of-Experts (MoEs) employ a conditional computation strategy where different submodules - so-called experts - are expected to be activated by different types of inputs. MoEs sees substantial success in various domains (Shen et al., 2023a; Chen et al., 2023b; Mustafa et al., 2022; Bao et al., 2022) in the era of large-scale transformers, and therefore becomes a widespread modular neural architecture.

Apart from developing *explicit* MNN, Csordás et al. (2021); Agarwala et al. (2021) study whether standard neural networks become *implicitly* modular after training and discover spontaneously emerged modular structure in small-scale CNNs and LSTMs. For more complicated large-scale pre-trained transformers, initial observations (Zhang et al., 2022b; Li et al., 2022) reveal notable

*Equal contribution.

†Work done while interning at HKUST.

‡Corresponding author

sparse activation patterns within the Feed-Forward Networks (FFNs). Specifically, they find that in T5-Base (Raffel et al., 2020) and ViT-B16, only 3.0% and 6.3% neurons are activated during one forward process. However, sparsity does not imply modularity. Sparsely activated FFNs neurons do not ensure to have remarkable functional division. Therefore, Zhang et al. (2023) further utilize handpicked semantic and knowledge-intensive tasks to probe the nature of neurons in FFNs. They observe a strong correlation between activation and specific tasks, further discovering clear function-based neuron grouping of the model and summarizing such phenomenon as *Emergent Modularity*.

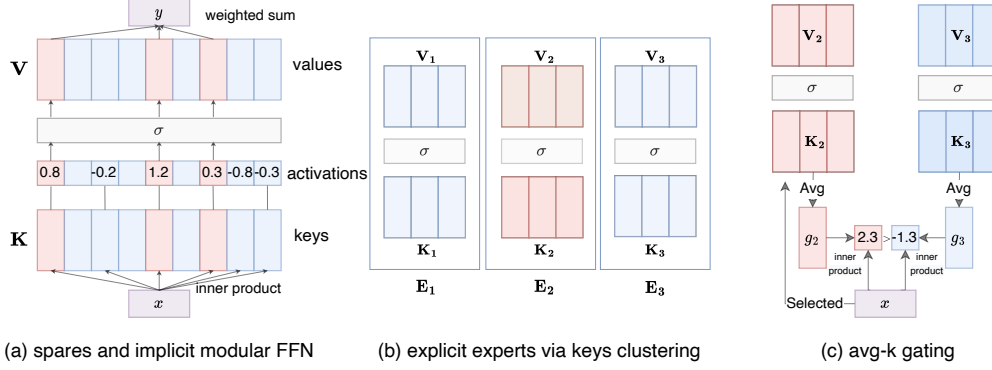


Figure 1: (a) Existing literatures (Geva et al., 2021; 2022) suggest that the FFNs in transformers can be viewed as key-value memories. They regarded the input as a query, the first layer as keys, and the second as values. Given an input, keys are sparsely activated (marked in red). Most of the values don't impact the output. (2) The FFNs block can be partitioned into experts by clustering keys. (3) Afterward, experts' keys averages are used as the gating weights. The inner product between x and gating weights are used to select experts.

However, contemporary transformers are still employed as monolithic models, with their emergent modularity underutilized. Motivated by the advantages of *explicit modularity*, we explore *whether and how standard pre-trained transformers could benefit from emergent modular structures*. Technically, we externalize the emergent modularity into the explicit MoEs, i.e., **Emergent Mixture-of-Experts** (EMoE). As shown in Figure 1, we first (1) utilize a clustering-based method to decompose the FFNs into experts and then (2) use the Average-Key-Gating (avg-k gating) to route the input to corresponding experts. Both two steps do not require extra training processes and data.

Then we fine-tune EMoE on a wide range of downstream tasks to investigate if standard pre-trained transformers can benefit from its emergent modular structure. We evaluate EMoE following different configurations: (1) tasks from various modalities: vision (Domainbed (Gulrajani & Lopez-Paz, 2021)) and language (GLUE (Wang et al., 2019) and GLUE-X (Yang et al., 2023)); (2) different pre-trained dense transformers: ViT (Dosovitskiy et al., 2021), BERT (Devlin et al., 2019), and GPT2 (Radford et al., 2019), ranging from 22M to 1.5B parameters. (3) different evaluation settings: in-domain (ID) evaluation and OOD evaluation; (4) different fine-tuning methods: full fine-tuning and parameter-efficient tuning (Hu et al., 2022). In total, we fine-tune **1785** models.

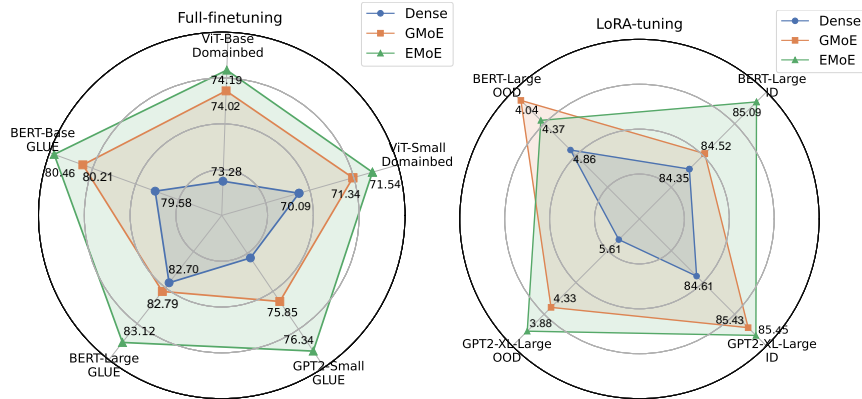


Figure 2: EMoE achieves stronger ID and OOD performances compared with baselines in both full-finetuning (Left, average accuracy) and LoRA tuning settings (Hu et al., 2022) (Right, average accuracy for ID and Friedman rank (Friedman, 1940) for OOD). Results are summarized from Section 4.

Our results are summarized in Figure 2. We find that **fine-tuning EMoE achieves significant improvement** compared with the vanilla fine-tuning and competitive performance with strong baseline GMoE (Li et al., 2023), demonstrating that dense pre-trained transformer can indeed benefit from emergent modular structures to achieve better generalization performance. We further find that **EMoE can deactivate neurons with negative transfer effects**, thus improving downstream performance. Meanwhile, our ablation studies indicate that EMoE’s insensitivity to various hyper-parameter configurations and higher data efficiency of up to 20%.

2 RELATED WORK

Modular neural networks has various advantages, including interpretability (Pfeiffer et al., 2023), scalability (Chowdhery et al., 2022), multi-task learning abilities (Chen et al., 2023a), and OOD generalization abilities (Goyal et al., 2021; Li et al., 2023). MoEs (Szymanski & Lemmon, 1993) is currently regarded as a standard framework for developing modular neural networks (Shen et al., 2023b). Most MoEs models are developed by training explicit MoEs architecture from random initialization (Shazeer et al., 2017; Fedus et al., 2022b; Zhang et al., 2022a), which usually causes load imbalance issues (Zoph et al., 2022; Fedus et al., 2022a; Chi et al., 2022). Some recent works employ already-trained dense models as a good initialization (Nie et al., 2021). For example, GMoE (Li et al., 2023) and Upcycling Komatsuaki et al. (2023) copy the FFNs from a trained dense network to continue pre-training or transfer learning. EMoE is also based on pre-trained dense models. However, unlike existing methods that often significantly increase in parameters (GMoE increases 50% parameters) or tend to be less effective (Upcycling extends T-5 Base (248M) to 2B parameters but still underperforms the T5-Large (783M)), EMoE achieves significant improvements without introducing extra training processes or parameters. This is primarily attributed to the heterogeneity of its experts and gating mechanisms, as we demonstrate in Section 5 and 6.

In another research line, Hod et al. (2021); Csordás et al. (2021) explore modular structures in CNNs and LSTMs. Some works (Zhang et al., 2022b; Li et al., 2022) focus on the sparsity of more complicated dense pre-trained transformers. Based on their observations, Zhang et al. (2023) recently explore modularity in pre-trained transformer FFNs. In this work, we adopt clustering-based expert construction and avg-k gating from MoEfication (Zhang et al., 2022b), while our motivation differs. Seeking to preserve the original functionality with fewer activated neurons, they split every layer in the dense model into MoEs. However, the results are worse than the dense model by more than ten points after splitting (Table 2 in their original paper). This is because the clustering-based decomposition and avg-k gating cannot precisely select the activated neurons. Without any tuning, these errors accumulate with MoEs layers and lead to severe performance dropping. Therefore, Zhang et al. (2022b) mainly focus on more complicated learning-based construction methods. Differently, we treat these decomposed units as heterogeneous modules to exploit their modular properties in the framework of MoEs, and observe significant improvements over monolithic models.

3 METHODOLOGY

3.1 PRELIMINARIES

Transformer Feed-Forward Networks The FFNs layer in the transformer block typically includes weights $\mathbf{K} \in \mathbb{R}^{d \times h}$, $\mathbf{V} \in \mathbb{R}^{h \times d}$, and a non-linear activation function $\sigma(\cdot)$. For an input $\mathbf{x} \in \mathbb{R}^h$, the output $\mathbf{y} \in \mathbb{R}^h$ can be calculated as follows:

$$\mathbf{y} = \text{FFN}(\mathbf{x}; \mathbf{K}, \mathbf{V}) = \sigma(\mathbf{x} \cdot \mathbf{K}^T) \cdot \mathbf{V}. \quad (1)$$

More precisely, for each row $\mathbf{K}_{i,:}$ and column $\mathbf{V}_{:,i}$, the Equation 1 can be rewritten as:

$$\mathbf{y} = \sigma(\mathbf{x} \cdot \mathbf{K}^T) \cdot \mathbf{V} = \sum_{i=1}^h \sigma(\mathbf{x} \cdot \mathbf{K}_{i,:}) \cdot \mathbf{V}_{:,i} \quad (2)$$

Regarding each row in \mathbf{K} as a key vector and each column in \mathbf{V} as the value vector, the output of an FFNs network can be viewed as a weighted sum of values based on the activation scores $\sigma(\mathbf{x} \cdot \mathbf{K}^T)$.

Mixture-of-Experts In transformers, MoEs is often implemented by replacing the original FFNs with a group of parallel FFNs and introducing a gating module. Supposing there are N experts:

$\{\text{FFN}_n(\cdot; \mathbf{K}^n, \mathbf{V}^n) | n \in [1, N]\}$, the gating module $g(\cdot; \mathbf{G}, k)$, defined with its parameters \mathbf{G} and an integer k , is to map input \mathbf{x} to a score distribution of experts $g(\mathbf{x}; \mathbf{G}, k) \in \mathcal{R}^N$. Typically, g is implemented with a simple linear layer followed by a softmax function and a Top-k function. Given an input $\mathbf{x} \in \mathbb{R}^h$, let $\mathbf{y}_n = \text{FFN}_n(\mathbf{x}; \mathbf{K}^n, \mathbf{V}^n)$ be the output of the n -th expert, and then the output $\mathbf{y} \in \mathbb{R}^h$ of can also be summarized as the weighted sum of the output from all experts:

$$\mathbf{y} = \sum_{n \in N} g_n(\mathbf{x}; \mathbf{G}, k) \text{FFN}_n(\mathbf{x}; \mathbf{K}^n, \mathbf{V}^n) = \sum_{n \in N} g_n(\mathbf{x}; \mathbf{G}, k) y_n, \quad (3)$$

When k for Top-K is smaller than N , only a subgroup of experts is involved in the computation.

3.2 EMERGENT MIXTURE-OF-EXPERT

The ideal EMoE should reflect the implicit modular nature of dense pre-trained transformers using the form of MoEs. A preferred approach to constructing EMoE should avoid introducing additional parameters, training, and data, which may result in undesired biases and are impractical. Although more sophisticated constructing methods can be proposed, we adopt a method from MoEfication [Zhang et al. \(2022b\)](#). The method contains two steps: (1) clustering-based expert construction and (2) avg-k gating. It is simple and fulfills our needs, as demonstrated in our experiments.

Clustering-based Experts Construction. Since key-value pairs with similar key vectors tend to be co-activated, we split them into separate experts according to their key vectors. Specifically, given a trained FFNs layer $\text{FFNs}(\cdot; \mathbf{K}, \mathbf{V})$, we perform constrained clustering ([Malinen & Fränti, 2014](#)) to partition all key vectors \mathbf{K} into N experts on average, so each group contains $\frac{d}{N}$ key-value pairs (usually $d = 4h$). Denoting the indices of keys in the i -th group as $E_i \subset [d]$, for $\forall j \in E_i$, we extract key-value pair $(\mathbf{K}_{j,:}, \mathbf{V}_{:,j})$ to form the i th expert $\text{FFN}(\cdot; \tilde{\mathbf{K}}_i, \tilde{\mathbf{V}}_i)$, as depicted in Figure 1(b). After that, the computation of each expert proceeds as Equation 1.

Avg-k Gating. Given an input \mathbf{x} and N experts, a qualified gate for EMoE should route the input \mathbf{x} to the experts who contribute most to the model’s output. We construct the gating module by averaging each expert’s keys. The gating function is usually implemented by a single layer $\mathbf{G} \in \mathcal{R}^{h \times N}$, in the avg-k gating’s case, the weights in n th column $\mathbf{G}_{:,n}$ can be calculated as follows:

$$\mathbf{G}_{:,n} = \text{Avg}(\mathbf{K}^n, \text{dim}=0). \quad (4)$$

And then the corresponding gating score for i -th expert is:

$$g_i(\mathbf{x}; \mathbf{G}, k) = \begin{cases} 1 & \text{if } i \in \text{Top-K}(\mathbf{x} \cdot \mathbf{G}^T; k, \text{dim}=1) \\ 0 & \text{else} \end{cases} \quad (5)$$

where $\text{Top-K}(\cdot; k, \text{dim})$ return indices of k largest element of the given input along a given dimension. Using 0,1 score, avg-k gating reduces the weights’ influence in Equation 3). Notably, observe:

$$\mathbf{x} \cdot \mathbf{G}_{:,n} = \mathbf{x} \cdot \text{Avg}(\mathbf{K}^n, \text{dim} = 0) = \mathbf{x} \cdot \frac{N}{h} \sum_{j \in E_i} \mathbf{K}_{j,:}^n = \frac{N}{h} \sum_j a_j. \quad (6)$$

A larger value of gating score g_i implies more activated keys within the corresponding expert. Consequently, the expert could potentially contribute more to the output \mathbf{y} for input \mathbf{x} . During downstream tuning, gating weights are updated along with the FFNs parameters using Equation 4.

3.3 DISCUSSION

Though adopting a method from MoEfication ([Zhang et al., 2022b](#)), EMoE has a distinct motivation, leading to different model configurations and testing scenarios. MoEfication applies the above method to each layer of fine-tuned models, hoping to boost inference efficiency by discarding inactivated neurons. However, the method introduces deviations from FFNs as it can mistakenly eliminate useful neurons. As these deviations accumulated across layers, the performances severely drop by over 10 points on original tasks. Therefore, they focus on more precise expert construction and gating to preserve performances. In sharp contrast, we treat the decomposed experts as heterogeneous modules and explore the benefits of such modularity in downstream tasks. We summarize their main differences in Appendix A.1. As one of our most related work, GMoE ([Li et al., 2023](#)) introduce MoEs by copying the trained FFNs. They further demonstrate introducing MoEs every 2 layers leads to significant degradation. Accordingly, we only introduce EMoEs in certain layers since efficiency isn’t our primary concern. We also conduct ablation studies about MoEfying every 2 layers and get consistent results, more details are in Appendix A.4.2 Table 14.

4 EXPERIMENTS

Experimental Configurations We evaluate EMoE on vision and language tasks. All experiments are repeated 3 times independently. We present the average in the main section, while full results are in Appendix A.4.1. Detail settings can be found in each experiment part. **Tasks and models:** In vision tasks, we employ ViT-Small (22M) and ViT-Base (86M) on 4 datasets from the Domainbed (Gulrajani & Lopez-Paz, 2021) for benchmarking vision OOD performance. In language tasks, we employ GLUE (Wang et al., 2019) and GLUE-X (Yang et al., 2023) for benchmarking language ID and OOD performance. We evaluate EMoE with a wide range of pre-trained language models, including BERT-Base/Large (110M/340M), and GPT2-Small/XL (124M/1.5B). For more details about datasets and evaluation metrics, please refer to the Appendix A.2. **Hyper-parameters:** those unrelated to MoEs, like the learning rate, remain consistent with the baselines. For others, guided by Li et al. (2023), we explore MoEs layers in {last two even layers, last one even layer}. Comparable hyper-parameter searches are conducted for both GMoE and EMoE for the number of experts N and top-k. In vision tasks, as highlighted by (Gulrajani & Lopez-Paz, 2021), the hyper-parameter search has a profound impact on outcomes. Consequently, we search with a relatively large scope: for GMoE, N is searched within {4, 6, 8}, and top-k within {2, 3, 4}; for EMoE, N is sought within {6, 12, 24}, and top-k within {2, 4, 8}. For Language tasks, GMoE explores N within {4, 8} and top-k within {1, 2}. For EMoE, N is fixed at 64, with top-k explored within {16, 32}. Our ablation study indicates that while hyper-parameter search yields superior performance, adhering to a top-k/ N = 0.5 for EMoE consistently brings improvement over dense counterparts.

Baselines On Domainbed, our baselines include (1) vanilla ViT, as it is a strong OOD baseline under fair configurations suggested by Gulrajani & Lopez-Paz (2021). (2) GMoE (Li et al., 2023), which is the latest state-of-the-art. GMoE constructs MoEs by replicating FFNs from the two-to-last and fourth-to-last transformer blocks of a pre-trained ViT and therefore is the most relevant to EMoE. For language tasks, besides vanilla backbone and GMoE, we implement (3) noisy tuning (Wu et al., 2022), which also improves adaptation for free by adding uniform distribution noise proportional to the standard deviation of the pre-trained weights before tuning. (4) EMoE-learn, an ablation method, where the gating function is learned (same as GMoE) during fine-tuning instead of employing avg-k gating. This helps us better understand the effect of avg-k gating.

Table 1: Overall OOD performances with 3 selection criteria. All the reported results are obtained following the Domainbed codebase. The best result is highlighted in **bold**. In cases where results are the same, the best result is determined by the smallest standard deviation. EMoE demonstrates comparable results to GMoE.

Results with ViT-small (22M) backbone						Results with ViT-base (86M) backbone					
Algorithm	PACS	VLCS	Office	Terra	Avg	Algorithm	PACS	VLCS	Office	Terra	Avg
Train-validation selection criterion						Train-validation selection criterion					
ViT	86.9	79.7	73.0	44.0	70.90	ViT	89.1	80.7	77.2	47.3	73.58
GMoE	87.7	79.6	73.1	45.4	71.45	GMoE	90.0	80.4	77.0	49.2	74.15
EMoE-learn	87.2	79.6	72.5	46.1	71.35	EMoE-learn	89.8	80.6	76.5	48.7	73.90
EMoE	87.8	79.5	73.1	45.9	71.58	EMoE	89.4	80.7	77.3	48.5	73.98
Leave-one-domain-out selection criterion						Leave-one-domain-out selection criterion					
ViT	86.1	79.7	73.3	45.0	71.03	ViT	88.9	80.8	77.5	46.1	73.33
GMoE	86.5	80.5	73.1	45.3	71.35	GMoE	89.3	81.0	76.7	50.1	74.28
EMoE-learn	86.8	79.6	72.6	45.8	71.20	EMoE-learn	89.3	81.2	76.5	50.5	74.38
EMoE	86.8	80.6	73.3	46.1	71.70	EMoE	89.6	81.6	77.4	50.0	74.65
Test-domain selection criterion						Test-domain selection criterion					
ViT	86.5	78.2	73.1	44.0	70.45	ViT	88.8	79.0	77.2	46.7	72.93
GMoE	87.2	79.0	73.4	45.3	71.23	GMoE	89.7	79.0	77.0	48.8	73.63
EMoE-learn	87.4	79.1	72.8	45.4	71.18	EMoE-learn	89.7	79.7	76.6	48.7	73.68
EMoE	87.6	79.0	73.3	45.5	71.35	EMoE	89.7	79.7	77.5	48.8	73.93

4.1 FULL FINE-TUNING PERFORMANCE

We test the EMoE’s OOD performance on Domainbed. Domainbed provides comprehensive vision OOD evaluations (one result is aggregated with 30 experiments), and the outcomes vary marginally. Moreover, Gulrajani & Lopez-Paz (2021) indicates that vanilla full fine-tuning with fair hyper-parameter search is a strong baseline compared with specifically designed methods like Invariant Risk Minimization (Arjovsky et al., 2019). More dataset details are in appendix A.2.1.

According to Table 1: (1) Overall, EMoE outperforms ViT and GMoE (except ViT-base Train-validation setting, upper right). (2) Compared with EMoE, EMoE-learn incorporates a learned gate. While it surpasses avg-k gating in certain scenarios (ViT-small Terra Train-validation), it can also lead to a performance drop compared with vanilla ViT. Its overall performance is lower than EMoE. (3) In tasks where the dense model is strong (like Office), EMoE performs better than other MoEs methods. One possible reason is that the avg-k gating reduces the influence of gating weights ($g_n(\mathbf{x}; \mathbf{G}; k)$ in Equation 3), making it more like the dense model in such scenarios.

Table 2: ID performance on GLUE tasks with different backbones and algorithms. All the reported results are obtained from 3 independent experiments. The average accuracy (Avg) is reported along with the relative improvement compared to the baseline. The best result is highlighted in **bold**.

Backbone	Algorithm	MRPC	CoLA	RTE	STSB	SST2	Avg
BERT Base	baseline	88.45	60.67	68.95	87.87	91.97	79.582
	noisy tuning	88.43	61.79	71.36	88.27	92.32	80.43(+0.85)
	GMoE	88.63	61.25	70.28	88.63	92.28	80.21(+0.63)
	EMoE-learn	89.05	62.46	70.40	88.47	92.58	80.59(+1.01)
	EMoE	89.45	61.55	69.68	88.71	92.89	80.46(+0.87)
BERT Large	baseline	89.82	65.41	74.89	89.87	93.50	82.70
	noisy tuning	90.42	64.75	73.41	90.05	93.65	82.46(-0.24)
	GMoE	91.24	64.90	74.24	90.00	93.58	82.79(+0.09)
	EMoE-learn	90.57	65.51	74.72	90.22	93.73	82.95(+0.25)
	EMoE	90.74	65.79	76.17	90.31	93.58	83.32(+0.62)
GPT2 Small	baseline	84.46	47.07	67.15	86.29	92.13	75.42
	noisy tuning	84.15	46.16	67.51	86.09	92.13	75.21(-0.21)
	GMoE	85.07	47.77	67.51	86.57	92.35	75.85(+0.43)
	EMoE-learn	85.73	47.24	67.99	86.66	92.35	75.99(+0.57)
	EMoE	85.40	48.00	68.95	86.64	92.70	76.34(+0.92)

We evaluate EMoE’s ID performance on 5 GLUE tasks. According to Table 2: (1) On average, EMoE and EMoE-learn outperform other baselines. (2) Among the two methods that do not introduce additional parameters, EMoE significantly outperforms noisy tuning. (3) EMoE provides stable improvements over baselines across different settings, demonstrating its generality.

4.2 LORA-TUNING PERFORMANCE

Table 3: ID and OOD performance of EMoE and baseline models. All the reported results are obtained from 3 independent experiments. OOD Metrics (averaged over 14 OOD tasks, lower is better) provide additional information for out-of-distribution generalization. The best result is highlighted in **bold**.

Algorithm	MRPC	CoLA	RTE	STSB	SST2	QNLI	QQP	MNLI	ID-Avg	OOD
BERT-Large (340M Parameters)										
LoRA	89.97	63.40	72.92	90.51	93.16	92.20	87.21	85.40	84.35	4.86
Block	89.34	62.10	71.96	90.39	93.35	92.04	88.45	86.20	84.23(-0.12)	4.95
GMoE	89.45	63.80	72.56	90.29	93.85	92.32	87.99	85.92	84.52(+0.18)	4.04
EMoE-block	89.77	63.25	71.60	90.31	93.69	92.09	88.08	86.21	84.38(+0.03)	5.89
EMoE-learn	89.87	64.00	71.36	90.48	93.65	92.40	87.55	85.62	84.37(+0.02)	4.66
EMoE	90.85	65.33	75.21	90.43	93.50	92.23	87.74	85.43	85.09(+0.74)	4.37
GPT2-XL (1.5B Parameters)										
LoRA	86.83	60.88	78.70	89.07	95.18	91.84	87.41	86.93	84.61	5.61
Block	86.59	61.18	79.78	89.08	95.45	91.88	87.71	86.95	84.83(+0.22)	5.13
GMoE	87.02	62.81	79.78	89.21	95.41	92.18	89.10	87.17	85.34(+0.73)	4.33
EMoE-block	87.86	62.88	80.05	89.18	95.49	92.10	89.69	86.87	85.52(+0.91)	5.71
EMoE-learn	87.93	61.50	79.90	89.48	95.18	92.33	89.71	87.00	85.38(+0.77)	4.40
EMoE	87.75	62.27	80.02	89.37	95.41	92.10	89.58	87.06	85.45(+0.84)	3.88

With the increasing scale of pre-trained models, parameter-efficient tuning (Houlsby et al., 2019) gets popular. Observing weaker results with LoRA-tuned ViT-Large on Domainbed compared to ViT-Base, we omit LoRA tuning on Domainbed. GLUE-X (Yang et al., 2023) is a recently introduced OOD dataset for the GLUE benchmark. Therefore, we assess EMoE’s ID performance on GLUE and OOD performance on GLUE-X with the standard LoRA tuning. Notably, LoRA weights are only added in attention, with all other weights frozen. Therefore, the only difference between EMoE and its dense counterpart is FFNs activation. For the *OOD metric*, we follow GLUE-X (Yang

et al., 2023) and employ the Friedman rank (Friedman, 1940) $\text{rank}_f = \frac{1}{n} \sum_{i=1}^n \text{rank}_i$. For each method under the same backbone, rank_i is produced based on the best result and the average result for each dataset. For the 13 OOD tasks used in GLUE-X, each method generates 26 rank_i values. The OOD results presented in Table 3 represent the mean of all these rank_i values. The original results of each task can be found in the Appendix A.4.1. For *algorithm configurations*, since GMoE copies the FFNs of the pre-trained model to form the MoEs, it is meaningless if the MoEs parameters aren't tuned. Thus, in Table 3, we conduct experiments with LoRA tuning for GMoE and also tune the transformer block where the original FFNs are replaced. For comparison, we also (1) LoRA-tune dense model and fine-tune the transformer block at the corresponding layer (denoted “Block”); (2) LoRA-tune EMoE with the transformed block also updated (denoted “EMoE-block”).

According to Table 3, EMoE continues to enhance the downstream performance in LoRA tuning: (1) EMoE demonstrates significant enhancements compared to LoRA and doesn't introduce additional trainable parameters or procedures. Notably, EMoE achieves comparable results with GMoE on BERT-large and outperforms it on GPT2-XL. (2) When the blocks are tuned, EMoE also brings improvements (EMoE-block vs. Block) (3) Consistent with the full-finetuning findings, EMoE exhibits higher stability than EMoE-learn and delivers superior overall results. (4) Besides vision, MoEs also improve OOD performance in language tasks (GMoE vs. Block, EMoE vs. LoRA).

5 ANALYSIS

5.1 HOW DOES EMOE IMPROVE FINE-TUNING PERFORMANCE?

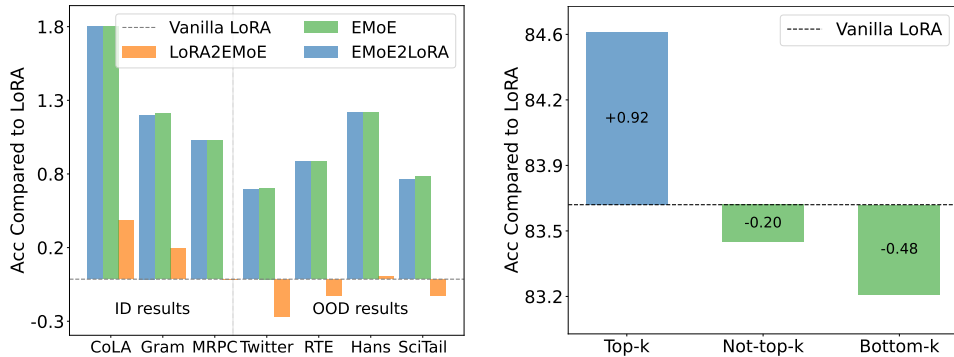


Figure 3: Left: ID and OOD results compared with LoRA for validating EMoE's training & inference effects. Right: sparse activated training results with different expert selections.

EMoE achieves notable improvements in both ID and OOD scenarios. However, it is non-trivial that simply transforming the pre-trained FFNs into MoEs before fine-tuning can yield such benefits (especially in LoRA tuning where the MoEs part is totally not updated). Therefore, we investigate the reasons behind the enhanced fine-tuning performance. *To decouple the impact of updating expert parameters, we focus on LoRA tuning.* We use BERT-Large as the backbone model.

EMoE benefits LoRA weights learning instead of influencing inference. EMoE and dense model only differ in FFNs activations; such difference might (1) directly impact outputs during testing and (2) influence the parameter updating during training. In light of this, we propose two variants and compare them with vanilla LoRA tuning and LoRA tuning with EMoE: (a) LoRA2EMoE: splitting a LoRA-tuned dense model into its MoEs counterpart. If the test results differ from the original ones, we can infer that the sparse activation has an impact during testing. (b) EMoE2LoRA: merging the LoRA weights tuned with EMoE back into the dense. If no changes occur, it implies that the primary factor is the parameter updating. According to Figure 3 Left, doing sparse activation during testing has little impact (LoRA2EMoE). But when merging LoRA weights tuned with EMoE back into the dense, the performance remains significantly better than the vanilla LoRA tuning (EMoE2LoRA vs. LoRA) and is almost identical to EMoE. For full results, please refer to Appendix A.4 Table 11.

EMoE masks neurons with negative transfer impacts. The only difference between EMoE and vanilla LoRA tuning is EMoE blocks some activated neurons during training by Top-k expert selection. Based on these, we hypothesize that EMoE's effects stem from preventing negative knowledge transfer from blocked neurons. Therefore, we investigate whether there are such negative transfers. Specifically, we study the following expert selection variants: (1) Bottom-k: select $k = 16$ experts

who get the lowest scores; (2) Not-top-k: select experts who are not among the top-k experts. These variants are evaluated across 6 tasks from GLUE. The averaged outcomes are in Figure 3 Right. Full results can be found in Appendix A.4 Table 12. LoRA tuning results with “Bottom-k” and “Not-top-k” expert selections are worse than vanilla LoRA tuning. One may attribute this drop to the reduced number of employed neurons. To further assess this, we compare “Top-k” with “Bottom-k”, where an equal number of neurons are used. Notably, “Bottom-k” significantly lags behind “Top-k”. This further corroborates that masked neurons have negative transfer effects.

5.2 ABLATION STUDIES

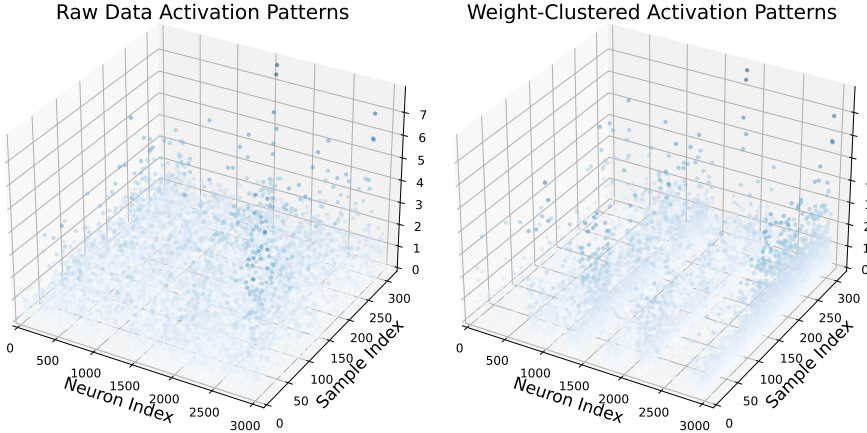


Figure 4: Left: Activations of neurons in FFNs a pre-trained ViT (Dosovitskiy et al., 2021). Right: By clustering the keys in the FFNs and rearranging the action values accordingly, activation patterns of neurons emerge. These co-activated patterns correspond to the modular structure within the pre-trained dense model. With appropriate partitioning, we can transform dense networks into modular networks.

Expert Constructing Methods Figure 4 demonstrates that clustering can decompose modular components within the dense model. To provide further evidence that the EMoE’s improvements stem from leveraging modular features rather than just sparse activation, we compare the results of (1) *clustering-based* expert construction and (2) *random* construction within the same setting of Section 5.1. The relative changes in averaged outcomes compared to the dense baseline are shown in Table 4, while full results can be found in the appendix A.4, Table 12. It’s noteworthy that while cluster top-k exhibits a significant improvement over dense, random top-k is conversely worse than dense baseline. This suggests that random construction can negatively impact gating. Moreover, considering selecting weights with negative transfer under bottom-k selections, it’s observed that cluster bottom-k also achieves lower results. In summary, clustering-based methods can externalize implicit modularity within the dense model. Within suitable frameworks like MoEs, such modularity can facilitate downstream tuning.

Table 4: Clustering-based and random expert constructing results

	Top-k	Bottom-K
Cluster	+0.92	-0.48
Random	-0.11	-0.34

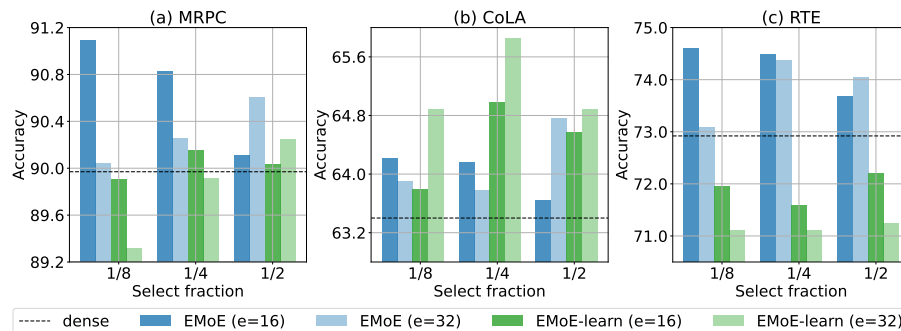


Figure 5: Results of 3 tasks for different experts splittings and expert select fractions (top-k / number of experts). ‘e=16’ and ‘e=32’ mean splitting FFNs into 16 and 32 experts, respectively.

Expert Constructing Configurations Beyond the settings detailed in the main results section, which are based on $N = 64$ experts and $\text{top-}k \in \{16, 32, 48\}$, we also present specific scenarios where $N \in \{16, 32\}$, and $\text{top-}k$ varies within $\{2, 4, 8, 16\}$ in Figure 5. Notably, in each of these settings, (1) EMoE consistently surpasses the dense model, illustrating its insensitivity to hyper-parameters. (2) On average, avg-k gating exhibits superior performance than learned gating. Though learned gating (EMoE-learn) outperforms avg-k gating in a few specific settings (Figure 5 (b) and (e)). This is consistent with the earlier results in Section 4. Regarding how many EMoE layers should be introduced, our findings align with those discovered in GMoE, indicating that only a limited number of layers can be converted into the EMoE layer. If excessive EMoE layers are introduced, performance deteriorates. Taking GPT2-XL (48 layers) as an example, when introducing EMoE every 2 layers in the latter half, the performance averaged across 5 GLUE tasks (79.36) matches that of the dense model (78.87). But when adopting EMoR every 2-layer for the entire model, the performance lags slightly behind that of the dense model (78.17) but surpasses EMoE-learn (75.87). For additional configurations, please refer to the appendix A.4.2 Table 14.

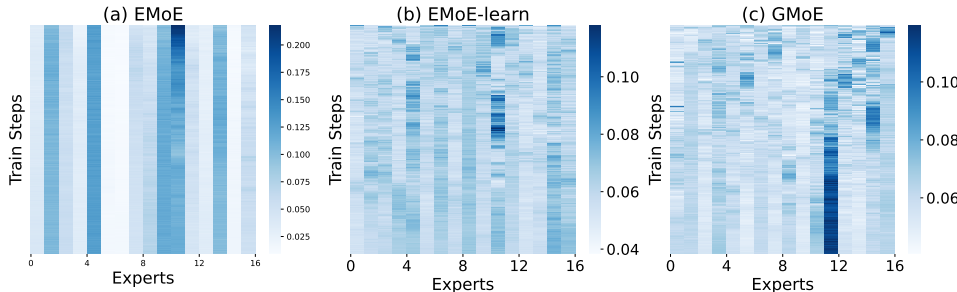


Figure 6: Expert selections during training with distinct gating functions (avg-k vs. learned) and expert types (modules from dense vs. repetitions of dense). The vertical axis illustrates training steps (top-down arrangement signifies begin-end); the horizontal axis represents expert selection frequency within 1K steps (deeper color implies a higher frequency). (a), (b) and (c) correspond to EMoE, EMoE-learn, and GMoE.

Expert Selection Changes During Training To further understand avg-k gating and learned gating, we visualize expert selections of GPT2-XL during fine-tuning on 6 tasks with 16 experts. In Figure 6, we showcase the results for the largest dataset QNLI among them. Full results are available in the appendix A.5. Our observations are: (1) Both avg-k gating and learned gating converge, as indicated by the lower halves of the plots. (2) avg-k gating is more stable than learned gating (Figure 6 a vs. b). This might mitigate data inefficiency from gating inconsistencies across different stages of training (Zuo et al., 2022). (3) EMoE, with its heterogeneous experts, exhibits better load balancing than GMoE (Figure 6 b vs. c). In GMoE, all experts share identical initialization, whereas in EMoE, the experts are derived from FFNs with implicit modularity. This also suggests a good initialization can facilitate MoEs learning similar to EvoMoE (Nie et al., 2021).

Performance Across Different Training set Volumes.

Previous research has indicated that modular architectures offer improved data efficiency (Bengio et al., 2020). Therefore, we conducted experiments with GPT2-XL on six tasks using varying proportions of original training data, and the results for all tasks are presented in Figure 7. It can be observed that EMoE consistently outperforms the dense across different data fractions. EMoE achieves superior results even when using less than 20% of the data. On SST2, only using 50% data, EMoE shows comparable performance to the dense. More details can be found in the Appendix A.4.2 Table 15. This further underscores the benefits of incorporating modular structures.

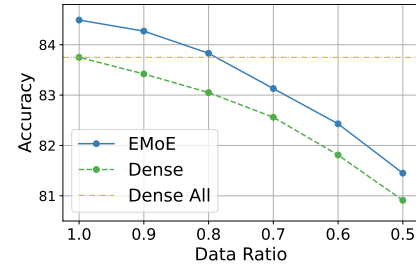


Figure 7: Average performance of EMoE with different proportions of training data.

6 CONCLUSION, LIMITATIONS AND FUTURE WORKS

Conclusion: In this work, we validate that exploiting the emergent modular structures in dense pre-trained transformers improves downstream task ID and OOD performances. One possible reason is

the modular structure can alleviate negative transfer effects presented in the pre-trained model. We hope our findings could deepen the understanding of neural networks’ modularity, further helping the community develop more sophisticated modular neural architectures and utilizing existing pre-trained models. **Limitations:** We would like to point out that EMoE is not designed to outperform the SOTA tuning methods and OOD generalization algorithms. Instead, the goal is to demonstrate that dense pre-trained transformers can benefit from emergent modular structures. Our research findings have not been validated on more challenging tasks (e.g., Mathematical Reasoning (Imani et al., 2023)) or foundation models like LLaMA (Touvron et al., 2023) due to computational constraints. While our evaluation was primarily conducted on models with a maximum parameter count of 1.5B, it is evident that across the spectrum of parameter sizes, ranging from 22M to 1.5B, EMoE consistently yields improvements, showing the potential to scale up. **Future works:** Subsequent research could delve into better methods for modular decomposition and investigate the modularity in foundation models. Benefiting from EMoE’s ability to avoid negative transfer, future researchers can also exploit the emergent modularity in settings such as multi-task learning and continual learning. Moreover, it is observed that modularity structures emergent and remain stable after approximately one-fourth of the pre-training phase (Li et al., 2022; Zhang et al., 2023). Future investigations could investigate leveraging the modularity of dense models during the pre-training process.

7 REPRODUCIBILITY

In the Experiment Configuration Section 4, we first introduce the additional configurations introduced by EMoE relative to the Dense Model, as well as the baseline settings. Subsequently, we provide high-level experiment settings for each experimental group (Domainbed at 4.1, full fine-tuning GLUE tasks at section 4.1, LoRA tuning at 4.2). In Appendix A.2, we provide detailed information on the datasets used, the codebase, and the evaluation metrics. We also outline more general configurations, such as learning rates and batch sizes for the respective tasks. Beyond the main paper, we include the original code for the experiments and log files for certain experimental results in the supplementary materials. Each section of code includes a README.md file that explains the experimental settings required to replicate the results.

REFERENCES

Atish Agarwala, Abhimanyu Das, Brendan Juba, Rina Panigrahy, Vatsal Sharan, Xin Wang, and Qiyu Zhang. One network fits all? modular versus monolithic task formulations in neural networks. In *9th International Conference on Learning Representations, ICLR 2021, Virtual Event, Austria, May 3-7, 2021*. OpenReview.net, 2021.

Jacob Andreas, Marcus Rohrbach, Trevor Darrell, and Dan Klein. Neural module networks. In *2016 IEEE Conference on Computer Vision and Pattern Recognition, CVPR 2016, Las Vegas, NV, USA, June 27-30, 2016*, pp. 39–48. IEEE Computer Society, 2016.

Martín Arjovsky, Léon Bottou, Ishaan Gulrajani, and David Lopez-Paz. Invariant risk minimization. *CoRR*, abs/1907.02893, 2019.

Gasser Auda and Mohamed S. Kamel. Modular neural networks A survey. *Int. J. Neural Syst.*, 9(2): 129–151, 1999.

Hangbo Bao, Wenhui Wang, Li Dong, Qiang Liu, Owais Khan Mohammed, Kriti Aggarwal, Subhajit Som, Songhao Piao, and Furu Wei. Vlmo: Unified vision-language pre-training with mixture-of-modality-experts. In *NeurIPS*, 2022.

Sara Beery, Grant Van Horn, and Pietro Perona. Recognition in terra incognita. In Vittorio Ferrari, Martial Hebert, Cristian Sminchisescu, and Yair Weiss (eds.), *Computer Vision - ECCV 2018 - 15th European Conference, Munich, Germany, September 8-14, 2018, Proceedings, Part XVI*, volume 11220 of *Lecture Notes in Computer Science*, pp. 472–489. Springer, 2018.

Yoshua Bengio, Tristan Deleu, Nasim Rahaman, Nan Rosemary Ke, Sébastien Lachapelle, Olexa Bilaniuk, Anirudh Goyal, and Christopher J. Pal. A meta-transfer objective for learning to disentangle causal mechanisms. In *8th International Conference on Learning Representations, ICLR 2020, Addis Ababa, Ethiopia, April 26-30, 2020*. OpenReview.net, 2020.

Zitian Chen, Mingyu Ding, Yikang Shen, Wei Zhan, Masayoshi Tomizuka, Erik G. Learned-Miller, and Chuang Gan. An efficient general-purpose modular vision model via multi-task heterogeneous training. *CoRR*, abs/2306.17165, 2023a.

Zitian Chen, Yikang Shen, Mingyu Ding, Zhenfang Chen, Hengshuang Zhao, Erik G. Learned-Miller, and Chuang Gan. Mod-squad: Designing mixtures of experts as modular multi-task learners. In *IEEE/CVF Conference on Computer Vision and Pattern Recognition, CVPR 2023, Vancouver, BC, Canada, June 17-24, 2023*, pp. 11828–11837. IEEE, 2023b.

Zewen Chi, Li Dong, Shaohan Huang, Damai Dai, Shuming Ma, Barun Patra, Saksham Singhal, Payal Bajaj, Xia Song, Xian-Ling Mao, Heyan Huang, and Furu Wei. On the representation collapse of sparse mixture of experts. In *NeurIPS*, 2022.

Aakanksha Chowdhery, Sharan Narang, Jacob Devlin, Maarten Bosma, Gaurav Mishra, Adam Roberts, Paul Barham, Hyung Won Chung, Charles Sutton, Sebastian Gehrmann, Parker Schuh, Kensen Shi, Sasha Tsvyashchenko, Joshua Maynez, Abhishek Rao, Parker Barnes, Yi Tay, Noam Shazeer, Vinodkumar Prabhakaran, Emily Reif, Nan Du, Ben Hutchinson, Reiner Pope, James Bradbury, Jacob Austin, Michael Isard, Guy Gur-Ari, Pengcheng Yin, Toju Duke, Anselm Levskaya, Sanjay Ghemawat, Sunipa Dev, Henryk Michalewski, Xavier Garcia, Vedant Misra, Kevin Robinson, Liam Fedus, Denny Zhou, Daphne Ippolito, David Luan, Hyeontaek Lim, Barret Zoph, Alexander Spiridonov, Ryan Sepassi, David Dohan, Shivani Agrawal, Mark Omernick, Andrew M. Dai, Thanumalayan Sankaranarayana Pillai, Marie Pellat, Aitor Lewkowycz, Erica Moreira, Rewon Child, Oleksandr Polozov, Katherine Lee, Zongwei Zhou, Xuezhi Wang, Brennan Saeta, Mark Diaz, Orhan Firat, Michele Catasta, Jason Wei, Kathy Meier-Hellstern, Douglas Eck, Jeff Dean, Slav Petrov, and Noah Fiedel. Palm: Scaling language modeling with pathways. *CoRR*, abs/2204.02311, 2022.

Róbert Csordás, Sjoerd van Steenkiste, and Jürgen Schmidhuber. Are neural nets modular? inspecting functional modularity through differentiable weight masks. In *9th International Conference on Learning Representations, ICLR 2021, Virtual Event, Austria, May 3-7, 2021*. OpenReview.net, 2021.

Jacob Devlin, Ming-Wei Chang, Kenton Lee, and Kristina Toutanova. BERT: pre-training of deep bidirectional transformers for language understanding. In Jill Burstein, Christy Doran, and Thamar Solorio (eds.), *Proceedings of the 2019 Conference of the North American Chapter of the Association for Computational Linguistics: Human Language Technologies, NAACL-HLT 2019, Minneapolis, MN, USA, June 2-7, 2019, Volume 1 (Long and Short Papers)*, pp. 4171–4186. Association for Computational Linguistics, 2019.

Alexey Dosovitskiy, Lucas Beyer, Alexander Kolesnikov, Dirk Weissenborn, Xiaohua Zhai, Thomas Unterthiner, Mostafa Dehghani, Matthias Minderer, Georg Heigold, Sylvain Gelly, Jakob Uszkoreit, and Neil Houlsby. An image is worth 16x16 words: Transformers for image recognition at scale. In *9th International Conference on Learning Representations, ICLR 2021, Virtual Event, Austria, May 3-7, 2021*. OpenReview.net, 2021.

Chen Fang, Ye Xu, and Daniel N. Rockmore. Unbiased metric learning: On the utilization of multiple datasets and web images for softening bias. In *IEEE International Conference on Computer Vision, ICCV 2013, Sydney, Australia, December 1-8, 2013*, pp. 1657–1664. IEEE Computer Society, 2013.

William Fedus, Jeff Dean, and Barret Zoph. A review of sparse expert models in deep learning. *CoRR*, abs/2209.01667, 2022a.

William Fedus, Barret Zoph, and Noam Shazeer. Switch transformers: Scaling to trillion parameter models with simple and efficient sparsity. *J. Mach. Learn. Res.*, 23:120:1–120:39, 2022b.

Milton Friedman. A comparison of alternative tests of significance for the problem of m rankings. *The annals of mathematical statistics*, 11(1):86–92, 1940.

Mor Geva, Roei Schuster, Jonathan Berant, and Omer Levy. Transformer feed-forward layers are key-value memories. In Marie-Francine Moens, Xuanjing Huang, Lucia Specia, and Scott Wen-tau Yih (eds.), *Proceedings of the 2021 Conference on Empirical Methods in Natural Language*

Processing, EMNLP 2021, Virtual Event / Punta Cana, Dominican Republic, 7-11 November, 2021, pp. 5484–5495. Association for Computational Linguistics, 2021.

Mor Geva, Avi Caciularu, Kevin Ro Wang, and Yoav Goldberg. Transformer feed-forward layers build predictions by promoting concepts in the vocabulary space. In Yoav Goldberg, Zornitsa Kozareva, and Yue Zhang (eds.), *Proceedings of the 2022 Conference on Empirical Methods in Natural Language Processing, EMNLP 2022, Abu Dhabi, United Arab Emirates, December 7-11, 2022*, pp. 30–45. Association for Computational Linguistics, 2022.

Anirudh Goyal and Yoshua Bengio. Inductive biases for deep learning of higher-level cognition. *CoRR*, abs/2011.15091, 2020.

Anirudh Goyal, Alex Lamb, Jordan Hoffmann, Shagun Sodhani, Sergey Levine, Yoshua Bengio, and Bernhard Schölkopf. Recurrent independent mechanisms. In *9th International Conference on Learning Representations, ICLR 2021, Virtual Event, Austria, May 3-7, 2021*. OpenReview.net, 2021.

Ishaan Gulrajani and David Lopez-Paz. In search of lost domain generalization. In *9th International Conference on Learning Representations, ICLR 2021, Virtual Event, Austria, May 3-7, 2021*. OpenReview.net, 2021.

Shlomi Hod, Stephen Casper, Daniel Filan, Cody Wild, Andrew Critch, and Stuart Russell. Detecting modularity in deep neural networks. *CoRR*, abs/2110.08058, 2021.

Neil Houlsby, Andrei Giurgiu, Stanislaw Jastrzebski, Bruna Morrone, Quentin de Laroussilhe, Andrea Gesmundo, Mona Attariyan, and Sylvain Gelly. Parameter-efficient transfer learning for NLP. In Kamalika Chaudhuri and Ruslan Salakhutdinov (eds.), *Proceedings of the 36th International Conference on Machine Learning, ICML 2019, 9-15 June 2019, Long Beach, California, USA*, volume 97 of *Proceedings of Machine Learning Research*, pp. 2790–2799. PMLR, 2019.

Edward J. Hu, Yelong Shen, Phillip Wallis, Zeyuan Allen-Zhu, Yuanzhi Li, Shean Wang, Lu Wang, and Weizhu Chen. Lora: Low-rank adaptation of large language models. In *The Tenth International Conference on Learning Representations, ICLR 2022, Virtual Event, April 25-29, 2022*. OpenReview.net, 2022.

Shima Imani, Liang Du, and Harsh Shrivastava. Mathprompter: Mathematical reasoning using large language models. In Sunayana Sitaram, Beata Beigman Klebanov, and Jason D. Williams (eds.), *Proceedings of the The 61st Annual Meeting of the Association for Computational Linguistics: Industry Track, ACL 2023, Toronto, Canada, July 9-14, 2023*, pp. 37–42. Association for Computational Linguistics, 2023.

Divyansh Kaushik, Eduard H. Hovy, and Zachary Chase Lipton. Learning the difference that makes A difference with counterfactually-augmented data. In *8th International Conference on Learning Representations, ICLR 2020, Addis Ababa, Ethiopia, April 26-30, 2020*. OpenReview.net, 2020.

Aran Komatsuzaki, Joan Puigcerver, James Lee-Thorp, Carlos Riquelme Ruiz, Basil Mustafa, Joshua Ainslie, Yi Tay, Mostafa Dehghani, and Neil Houlsby. Sparse upcycling: Training mixture-of-experts from dense checkpoints. In *The Eleventh International Conference on Learning Representations, ICLR 2023, Kigali, Rwanda, May 1-5, 2023*. OpenReview.net, 2023.

Bo Li, Yifei Shen, Jingkang Yang, Yezhen Wang, Jiawei Ren, Tong Che, Jun Zhang, and Ziwei Liu. Sparse mixture-of-experts are domain generalizable learners. In *The Eleventh International Conference on Learning Representations, ICLR 2023, Kigali, Rwanda, May 1-5, 2023*. OpenReview.net, 2023.

Da Li, Yongxin Yang, Yi-Zhe Song, and Timothy M. Hospedales. Deeper, broader and artier domain generalization. *CoRR*, abs/1710.03077, 2017.

Zonglin Li, Chong You, Srinadh Bhojanapalli, Daliang Li, Ankit Singh Rawat, Sashank J. Reddi, Ke Ye, Felix Chern, Felix X. Yu, Ruiqi Guo, and Sanjiv Kumar. Large models are parsimonious learners: Activation sparsity in trained transformers. *CoRR*, abs/2210.06313, 2022.

Andrew L. Maas, Raymond E. Daly, Peter T. Pham, Dan Huang, Andrew Y. Ng, and Christopher Potts. Learning word vectors for sentiment analysis. In Dekang Lin, Yuji Matsumoto, and Rada Mihalcea (eds.), *The 49th Annual Meeting of the Association for Computational Linguistics: Human Language Technologies, Proceedings of the Conference, 19-24 June, 2011, Portland, Oregon, USA*, pp. 142–150. The Association for Computer Linguistics, 2011.

Mikko I. Malinen and Pasi Fränti. Balanced k-means for clustering. In Pasi Fränti, Gavin Brown, Marco Loog, Francisco Escolano, and Marcello Pelillo (eds.), *Structural, Syntactic, and Statistical Pattern Recognition - Joint IAPR International Workshop, S+SSPR 2014, Joensuu, Finland, August 20-22, 2014. Proceedings*, volume 8621 of *Lecture Notes in Computer Science*, pp. 32–41. Springer, 2014.

Basil Mustafa, Carlos Riquelme, Joan Puigcerver, Rodolphe Jenatton, and Neil Houlsby. Multi-modal contrastive learning with limoe: the language-image mixture of experts. In *NeurIPS*, 2022.

Xiaonan Nie, Xupeng Miao, Shijie Cao, Lingxiao Ma, Qibin Liu, Jilong Xue, Youshan Miao, Yi Liu, Zhi Yang, and Bin Cui. Evomoe: An evolutional mixture-of-experts training framework via dense-to-sparse gate. *arXiv preprint arXiv:2112.14397*, 2021.

Jonas Pfeiffer, Sebastian Ruder, Ivan Vulic, and Edoardo Maria Ponti. Modular deep learning. *CoRR*, abs/2302.11529, 2023.

Alec Radford, Jeffrey Wu, Rewon Child, David Luan, Dario Amodei, Ilya Sutskever, et al. Language models are unsupervised multitask learners. *OpenAI blog*, 1(8):9, 2019.

Colin Raffel, Noam Shazeer, Adam Roberts, Katherine Lee, Sharan Narang, Michael Matena, Yanqi Zhou, Wei Li, and Peter J. Liu. Exploring the limits of transfer learning with a unified text-to-text transformer. *J. Mach. Learn. Res.*, 21:140:1–140:67, 2020.

Noam Shazeer, Azalia Mirhoseini, Krzysztof Maziarz, Andy Davis, Quoc V. Le, Geoffrey E. Hinton, and Jeff Dean. Outrageously large neural networks: The sparsely-gated mixture-of-experts layer. In *5th International Conference on Learning Representations, ICLR 2017, Toulon, France, April 24-26, 2017, Conference Track Proceedings*. OpenReview.net, 2017.

Sheng Shen, Zhewei Yao, Chunyuan Li, Trevor Darrell, Kurt Keutzer, and Yuxiong He. Scaling vision-language models with sparse mixture of experts. *CoRR*, abs/2303.07226, 2023a.

Yikang Shen, Zheyu Zhang, Tianyou Cao, Shawn Tan, Zhenfang Chen, and Chuang Gan. Moduleformer: Learning modular large language models from uncurated data. *CoRR*, abs/2306.04640, 2023b.

Peter T. Szymanski and Michael D. Lemmon. Adaptive mixtures of local experts are source coding solutions. In *Proceedings of International Conference on Neural Networks (ICNN'88), San Francisco, CA, USA, March 28 - April 1, 1993*, pp. 1391–1396. IEEE, 1993.

Hugo Touvron, Thibaut Lavril, Gautier Izacard, Xavier Martinet, Marie-Anne Lachaux, Timothée Lacroix, Baptiste Rozière, Naman Goyal, Eric Hambro, Faisal Azhar, Aurélien Rodriguez, Armand Joulin, Edouard Grave, and Guillaume Lample. Llama: Open and efficient foundation language models. *CoRR*, abs/2302.13971, 2023.

Nirali Vaghani and Mansi Thummar. Flipkart product reviews with sentiment dataset, 2023.

Hemanth Venkateswara, Jose Eusebio, Shayok Chakraborty, and Sethuraman Panchanathan. Deep hashing network for unsupervised domain adaptation. In *2017 IEEE Conference on Computer Vision and Pattern Recognition, CVPR 2017, Honolulu, HI, USA, July 21-26, 2017*, pp. 5385–5394. IEEE Computer Society, 2017.

Alex Wang, Amanpreet Singh, Julian Michael, Felix Hill, Omer Levy, and Samuel R. Bowman. GLUE: A multi-task benchmark and analysis platform for natural language understanding. In *7th International Conference on Learning Representations, ICLR 2019, New Orleans, LA, USA, May 6-9, 2019*. OpenReview.net, 2019.

Martin Weiss, Nasim Rahaman, Francesco Locatello, Chris Pal, Yoshua Bengio, Bernhard Schölkopf, Li Erran Li, and Nicolas Ballas. Neural attentive circuits. In *NeurIPS*, 2022.

Chuhan Wu, Fangzhao Wu, Tao Qi, and Yongfeng Huang. Noisytune: A little noise can help you finetune pretrained language models better. In Smaranda Muresan, Preslav Nakov, and Aline Villavicencio (eds.), *Proceedings of the 60th Annual Meeting of the Association for Computational Linguistics (Volume 2: Short Papers), ACL 2022, Dublin, Ireland, May 22-27, 2022*, pp. 680–685. Association for Computational Linguistics, 2022.

Linyi Yang, Shuibai Zhang, Libo Qin, Yafu Li, Yidong Wang, Hanmeng Liu, Jindong Wang, Xing Xie, and Yue Zhang. GLUE-X: evaluating natural language understanding models from an out-of-distribution generalization perspective. In Anna Rogers, Jordan L. Boyd-Graber, and Naoaki Okazaki (eds.), *Findings of the Association for Computational Linguistics: ACL 2023, Toronto, Canada, July 9-14, 2023*, pp. 12731–12750. Association for Computational Linguistics, 2023.

Xiang Zhang, Junbo Jake Zhao, and Yann LeCun. Character-level convolutional networks for text classification. In Corinna Cortes, Neil D. Lawrence, Daniel D. Lee, Masashi Sugiyama, and Roman Garnett (eds.), *Advances in Neural Information Processing Systems 28: Annual Conference on Neural Information Processing Systems 2015, December 7-12, 2015, Montreal, Quebec, Canada*, pp. 649–657, 2015.

Xiaofeng Zhang, Yikang Shen, Zeyu Huang, Jie Zhou, Wenge Rong, and Zhang Xiong. Mixture of attention heads: Selecting attention heads per token. In *Proceedings of the 2022 Conference on Empirical Methods in Natural Language Processing, EMNLP 2022, Abu Dhabi, United Arab Emirates, December 7-11, 2022*, pp. 4150–4162. Association for Computational Linguistics, 2022a.

Zhengyan Zhang, Yankai Lin, Zhiyuan Liu, Peng Li, Maosong Sun, and Jie Zhou. Moefication: Transformer feed-forward layers are mixtures of experts. In Smaranda Muresan, Preslav Nakov, and Aline Villavicencio (eds.), *Findings of the Association for Computational Linguistics: ACL 2022, Dublin, Ireland, May 22-27, 2022*, pp. 877–890. Association for Computational Linguistics, 2022b.

Zhengyan Zhang, Zhiyuan Zeng, Yankai Lin, Chaojun Xiao, Xiaozhi Wang, Xu Han, Zhiyuan Liu, Ruobing Xie, Maosong Sun, and Jie Zhou. Emergent modularity in pre-trained transformers. In Anna Rogers, Jordan L. Boyd-Graber, and Naoaki Okazaki (eds.), *Findings of the Association for Computational Linguistics: ACL 2023, Toronto, Canada, July 9-14, 2023*, pp. 4066–4083. Association for Computational Linguistics, 2023.

Barret Zoph, Irwan Bello, Sameer Kumar, Nan Du, Yanping Huang, Jeff Dean, Noam Shazeer, and William Fedus. St-moe: Designing stable and transferable sparse expert models. *arXiv preprint arXiv:2202.08906*, 2022.

Simiao Zuo, Xiaodong Liu, Jian Jiao, Young Jin Kim, Hany Hassan, Ruofei Zhang, Jianfeng Gao, and Tuo Zhao. Taming sparsely activated transformer with stochastic experts. In *The Tenth International Conference on Learning Representations, ICLR 2022, Virtual Event, April 25-29, 2022*. OpenReview.net, 2022.

A APPENDIX

A.1 COMPARE WITH MOEFICATION

Table 5: Comparison between EMoE and Moefication

Aspect	EMoE	Moefication
Motivation	Modularity	Sparsity
Goal	Transfer learning effective	Inference efficiency
MoEs Layers	Typically 1 or 2 layers	Applies changes across all layers
Scenarios	Down-stream tasks	Original task
Results	Significant improvement without adding parameters	Improved inference efficiency but performance drop

Though adopting the MoEs construction method from MoEfication (Zhang et al., 2022b), EMoE has a distinct motivation, leading to different model configurations and testing scenarios. MoEfication applies the above method to each layer of fine-tuned models, hoping to boost inference efficiency by discarding inactivated neurons. In sharp contrast, we treat the decomposed experts as heterogeneous modules and explore the benefits of such modularity in downstream tasks. Accordingly, We only introduce EMoEs in certain layers according to GMoE, since efficiency is not our primary concern. These differences are summarized in Table 5.

A.2 DATASETS AND EVALUATION METRICS

A.2.1 DOMAINBED

Table 6: Used dataset information from Domainbed

Dataset	PACS	VLCS	OfficeHome	TerraInc
#Domains	4	4	4	4
Classes	7	5	65	10
Images	9,991	10,729	15,588	24,788

The four datasets (PACS (Li et al., 2017), VLCS (Fang et al., 2013), Office-Home (Venkateswara et al., 2017), and Terra Incognita (Beery et al., 2018)) are selected from Domainbed. Each dataset comprises 4 distinct domains(PACS: {art, cartoons, photos, sketches}, VLCS: {Caltech101, LabelMe, SUN09, VOC2007}, Office-Home: {art,clipart, product, real}, and Terra Incognita: {L100, L38, L48, L46}). Within a single training, one or two domains’ data are sequentially designated for OOD evaluation. For example, when training on PACS, {art, cartoons} could be selected as ID training data, while {photos, sketches} are designated for OOD testing. This configuration results in a total of $C_4^2 + C_4^1 = 10$ distinct training processes within each dataset. Suppose there are d_{tr} ID domains, “Train-validation” means selecting OOD test checkpoints based on ID accuracies from the validation subsets of all d_{tr} ID domains; “Leave-one-domain-out” means leaving one selected ID domain as a validation set, doing training on $d_{tr} - 1$ domains; “Test-domain” means selection based on limited accesses to test domains and selecting based on these results. The final results are aggregated with selection criteria provided by Domainbed¹. As a result, even a variation of 0.1 in the benchmark outcomes signifies a significant improvement.

In our experiments, all the hyper-parameters, like training steps, learning rates, and weight decay, except those related to MoEs, strictly follow GMoE.

A.2.2 GLUE

Each task involves one to four OOD tasks from GLUE-X (Yang et al., 2023), resulting in 13 OOD tasks in total. To illustrate, consider the Sentiment Analysis task: we first fine-tune models on SST-2 from GLUE and report the validation results as ID performance, then use the test data from IMDB (Maas et al., 2011), Yelp (Zhang et al., 2015), Amazon (Kaushik et al., 2020) and Flipkart (Vaghani & Thummar, 2023) from GLUE-X for OOD testing.

In the *full fine-tuning*, to ensure convergence and reduce randomness, we train all models 10 epochs across 3 random seeds on each task. Each experiment does a hyper-parameter search on learning rates on [2e-5, 3e-5, 5e-5] as suggested by BERT (Devlin et al., 2019). The training batch size is 32. In the *LoRA tuning*, following LoRA (Hu et al., 2022) that tunes models with more epochs and larger learning rates than standard full fine-tuning, all models are trained 20 epochs on small and medium datasets and 5 epochs on large ones (like QNLI, MNLI, QQP). The learning rate is searched in [2e-4, 3e-4, 5e-4]. All methods are implemented with LoRA_rank=8 and LoRA_alpha=16. The training batch size is 16 due to a larger model size. Other settings like max_length following the codebase from hugging face². After training on GLUE, we directly test the selected models on GLUE-X with the data from the official repo³.

¹<https://github.com/facebookresearch/DomainBed>

²<https://github.com/huggingface/transformers/tree/main/examples/pytorch/text-classification>

³<https://github.com/YangLinyi/GLUE-X>

Table 7: Language tasks and corresponding ID and OOD datasets.

Task	ID-dataset	size	OOD-dataset	size
Paraphrase	MRPC	4,076	Twitter	16,777
	QQP	404,301	Twitter MRPC	16,777 4,076
Linguistic Acceptability	CoLA	9,594	Grammar Test	304,277
Textual Entailment	RTE	2,768	SciTail HANs	26,527 60,000
Textual Similarity	STSB	7,128	SICK	9,840
Sentiment Analysis	SST2	68,223	IMDB	50,000
			Yelp	598,000
			Amazon	4,000,000
			Flipkart	205,041
Question Answering NLI	QNLI	110,206	NewsQA	119,525
Natural Language Inference	MNLI	412,313	SICK	9,840

A.3 COMPUTATION COST AND MEMORY USAGE

Theoretically, EMoE does not introduce additional parameters compared to its dense counterpart. Although it adds computation in the gating portion within the MoEs layer, it omits a substantial amount of computation within the FFNs layer. For instance, the computation in the gating portion is of the order of $h \times N$, where h represents the model’s hidden size, and N is the number of experts. In contrast, the complete computation in the FFNs layer is of the order of $(h \times h \times 4h) \times 2$, and sparse activations can reduce more than a quarter of this computation. Since $N \ll h$, theoretically, using EMoE within a single block should accelerate the forward pass of the model. However, in real deployment, we have observed that the hardware implementation of MoEs can result in EMoE being, on average, approximately 10% slower than the dense model. Additionally, the memory usage is also slightly higher, by less than 5%, compared to the dense model (16295MB v.s. 15865MB on CoLA, LoRA tuning GPT2-XL).

Each individual experiment was conducted on a single NVIDIA 40G A100 GPU. The training times for different tasks ranged from just over ten minutes (RTE) to more than ten hours (QQP).

A.4 TABULAR RESULTS

A.4.1 FULL TABLES IN FULL FINE-TUNING WITH STANDARD DEVIATION

In this section, we present the mean and variance of experiments conducted with three different random seeds. The Domainbed results are demonstrated in Table 8, full fine-tuning results are in Table 9, LoRA tuning results are in Table 10.

A.4.2 FULL TABLES AND FIGURE DATA SOURCES IN ANALYSIS

In the Analysis section 5.1, for the sake of clarity, we have transformed tabular data into graphs or retained only a subset of the results. The original and complete results corresponding to them are presented in this section. Figure 3 is summarized from Table 11 and Table 12. The OOD results in Table 3 are from 10. The ablation studies are from Table 14 and Table 15.

A.5 MORE VISUALIZATION RESULTS

In this part, we demonstrate more gating visualization results on SST-2, STSB, MRPC, and RTE in Figure 8. These results are consistent with earlier findings: (1) Both avg-k gating and learned gating converge, as indicated by the lower halves of the plots. (2) avg-k gating is more stable than learned

Table 8: Overall out-of-domain performances with different selection criteria. All the reported results are obtained from three independent experiments conducted following the Domainbed codebase. The best result is highlighted in **bold**. In cases where results are the same, the best result is determined by the smallest standard deviation. EMoE demonstrates comparable results to GMoE.

Results with ViT-small backbone						Results with ViT-base backbone					
Algorithm	PACS	VLCS	OfficeHome	TerraInc	Avg	Algorithm	PACS	VLCS	OfficeHome	TerraInc	Avg
train-validation selection criterion						train-validation selection criterion					
ViT	86.9 \pm 0.2	79.7\pm0.4	73.0 \pm 0.2	44.0 \pm 1.1	70.90	ViT	89.1 \pm 0.0	80.7\pm0.1	77.2 \pm 0.1	47.3 \pm 0.8	73.58
GMoE	87.7 \pm 0.2	79.6 \pm 0.4	73.1 \pm 0.3	45.4 \pm 0.3	71.45	GMoE	90.0\pm0.3	80.4 \pm 0.6	77.0 \pm 0.1	49.2\pm1.1	74.15
EMoE-learn	87.2 \pm 0.4	79.6 \pm 0.2	72.5 \pm 0.2	46.1\pm0.4	71.35	EMoE-learn	89.8 \pm 0.2	80.6 \pm 0.2	76.5 \pm 0.1	48.7 \pm 0.5	73.90
EMoE	87.8\pm0.2	79.5 \pm 0.4	73.1\pm0.2	45.9 \pm 0.3	71.58	EMoE	89.4 \pm 0.4	80.7 \pm 0.2	77.3\pm0.1	48.5 \pm 0.5	73.98
leave-one-domain-out selection criterion						leave-one-domain-out selection criterion					
ViT	86.1 \pm 0.6	79.7 \pm 0.4	73.3\pm0.1	45.0 \pm 0.5	71.03	ViT	88.9 \pm 0.4	80.8 \pm 0.3	77.5\pm0.1	46.1 \pm 0.6	73.33
GMoE	86.5 \pm 0.3	80.5 \pm 0.2	73.1 \pm 0.3	45.3 \pm 0.6	71.35	GMoE	89.3 \pm 0.6	81.0 \pm 0.3	76.7 \pm 0.1	50.1 \pm 1.1	74.28
EMoE-learn	86.8\pm0.0	79.6 \pm 0.3	72.6 \pm 0.2	45.8 \pm 0.6	71.20	EMoE-learn	89.3 \pm 0.2	81.2 \pm 0.1	76.5 \pm 0.1	50.5\pm0.2	74.38
EMoE	86.8 \pm 0.1	80.6\pm0.4	73.3 \pm 0.2	46.1\pm0.6	71.70	EMoE	89.6\pm0.2	81.6\pm0.2	77.4 \pm 0.1	50.0 \pm 1.1	74.65
test-domain selection criterion						test-domain selection criterion					
ViT	86.5 \pm 0.4	78.2 \pm 0.4	73.1\pm0.2	44.0 \pm 0.5	70.45	ViT	88.8 \pm 0.7	79.0 \pm 0.5	77.2 \pm 0.0	46.7 \pm 0.4	72.93
GMoE	87.2 \pm 0.4	79.0 \pm 0.3	73.4\pm0.2	45.3 \pm 0.4	71.23	GMoE	89.7 \pm 0.5	79.0 \pm 0.3	77.0 \pm 0.1	48.8\pm0.4	73.63
EMoE-learn	87.4 \pm 0.2	79.1\pm0.3	72.8 \pm 0.1	45.4 \pm 0.6	71.18	EMoE-learn	89.7\pm0.4	79.7\pm0.2	76.6 \pm 0.1	48.7 \pm 0.3	73.68
EMoE	87.6\pm0.5	79.0 \pm 0.2	73.3 \pm 0.0	45.5\pm0.1	71.35	EMoE	89.7\pm0.4	79.7\pm0.2	77.5\pm0.1	48.8 \pm 0.6	73.93

Table 9: Results on GLUE tasks with different backbones and algorithms. All the reported results are obtained from 3 independent experiments. The average accuracy (avg) is reported along with the relative improvement compared to the baseline. The best result is highlighted in **bold**.

Backbone	Algorithm	MRPC	CoLA	RTE	STSB	SST2	Avg
BERT-B	baseline	88.45 \pm 0.40	60.67 \pm 0.54	68.95 \pm 0.69	87.87 \pm 0.12	91.97 \pm 0.19	79.582
	noisy tuning	88.43 \pm 0.12	61.79 \pm 0.16	71.36 \pm 0.17	88.27 \pm 0.94	92.32 \pm 0.25	80.43(+0.85)
	GMoE	88.63 \pm 0.53	61.25 \pm 2.36	70.28 \pm 0.68	88.63 \pm 0.65	92.28 \pm 0.24	80.21(+0.63)
	EMoE-learn	89.05 \pm 0.23	62.46\pm1.01	70.40\pm1.28	88.47 \pm 0.74	92.58 \pm 0.14	80.59(+1.01)
	EMoE	89.45\pm0.36	61.55 \pm 0.67	69.68 \pm 1.02	88.71\pm0.50	92.89\pm0.19	80.46(+0.87)
BERT-L	baseline	89.82 \pm 1.30	65.41 \pm 0.47	74.89 \pm 1.39	89.87 \pm 0.28	93.50 \pm 0.24	82.70
	noisy tuning	90.42 \pm 0.35	64.75 \pm 1.31	73.41 \pm 1.62	90.05 \pm 0.46	93.65 \pm 0.11	82.46(-0.24)
	GMoE	91.24\pm0.25	64.90 \pm 1.26	74.24 \pm 1.04	90.00 \pm 0.64	93.58 \pm 0.25	82.79(+0.09)
	EMoE-learn	90.57 \pm 0.43	65.51 \pm 0.32	74.72 \pm 2.13	90.22 \pm 0.49	93.73\pm0.35	82.95(+0.25)
	EMoE	90.74 \pm 0.65	65.79\pm1.16	76.17\pm0.00	90.31\pm0.43	93.58 \pm 0.32	83.32(+0.62)
GPT2	baseline	84.46 \pm 0.51	47.07 \pm 1.60	67.15 \pm 0.51	86.29 \pm 0.29	92.13 \pm 0.30	75.42
	noisy tuning	84.15 \pm 0.92	46.16 \pm 2.79	67.51 \pm 0.78	86.09 \pm 0.38	92.13 \pm 0.27	75.21(-0.21)
	GMoE	85.07 \pm 0.45	47.77 \pm 3.20	67.51 \pm 0.51	86.57 \pm 0.29	92.35 \pm 0.35	75.85(+0.43)
	EMoE-learn	85.73\pm0.09	47.24 \pm 1.48	67.99 \pm 0.17	86.66\pm0.32	92.35 \pm 0.38	75.99(+0.57)
	EMoE	85.40 \pm 0.77	48.00\pm1.50	68.95\pm0.29	86.64 \pm 0.16	92.70\pm0.22	76.34(+0.92)

gating. This could mitigate data inefficiency resulting from inconsistencies in gating across different stages of training (Zuo et al., 2022).

Table 10: Results on various algorithms with different models and tasks. All the reported results are obtained from 3 independent experiments. OOD Metrics (averaged over 14 OOD tasks, lower is better) provide additional information for out-of-distribution generalization. The best result is highlighted in **bold**, and the second is marked with underline.

Algorithm	MRPC	CoLA	RTE	STSB	SST2	QNLI	QQP	MNLI	ID-Avg	OOD
BERT-Large (340 Million Parameters) Results										
LoRA	89.97 \pm 0.40	63.40 \pm 0.62	72.92 \pm 1.64	90.51 \pm 0.18	93.16 \pm 0.19	92.20 \pm 0.13	87.21 \pm 0.60	85.40 \pm 0.07	84.35	4.86
Block	89.34 \pm 0.84	62.10 \pm 0.91	71.96 \pm 1.68	90.39 \pm 0.14	93.35 \pm 0.43	92.04 \pm 0.16	88.45 \pm 0.07	86.20 \pm 0.10	84.23(-0.12)	4.95
Block+GMoE	89.45 \pm 0.72	63.80 \pm 0.71	72.56 \pm 0.29	90.29 \pm 0.07	93.85\pm0.11	92.32 \pm 0.14	87.99 \pm 0.06	85.92 \pm 0.13	84.52(+0.18)	4.04
Block+EMoE-learn	89.79 \pm 0.23	64.16 \pm 0.87	73.16 \pm 1.04	90.27 \pm 0.03	93.85\pm0.11	92.40 \pm 0.06	88.01 \pm 0.12	85.76 \pm 0.19	84.68(+0.33)	3.94
Block+EMoE	89.77 \pm 0.46	63.25 \pm 0.50	71.60 \pm 0.68	90.31 \pm 0.09	93.69 \pm 0.32	92.09 \pm 0.13	88.08 \pm 0.19	86.21\pm0.16	84.38(+0.03)	5.89
EMoE	90.85\pm0.61	65.33\pm0.40	75.21\pm1.62	90.43 \pm 0.06	93.50 \pm 0.33	92.23 \pm 0.10	87.74 \pm 0.10	85.43 \pm 0.10	85.09(+0.74)	4.37
EMoE+LN	90.47 \pm 0.33	64.39 \pm 0.31	73.41 \pm 1.04	90.54\pm0.03	93.00 \pm 0.16	92.31 \pm 0.05	88.79\pm0.17	85.50 \pm 0.10	84.80(+0.46)	4.53
EMoE-learn	89.87 \pm 0.50	64.00 \pm 0.57	71.36 \pm 1.39	90.48 \pm 0.10	93.65 \pm 0.33	92.40\pm0.11	87.55 \pm 0.14	85.62 \pm 0.23	84.37(+0.02)	4.66
EMoE-learn+LN	89.99 \pm 0.25	64.16 \pm 1.16	72.44 \pm 0.45	90.45 \pm 0.10	93.42 \pm 0.38	92.15 \pm 0.10	87.70 \pm 0.04	85.52 \pm 0.24	84.47(0.12)	4.28
GPT2-XL (1.5 Billion Parameters) Results										
LoRA	86.83 \pm 0.87	60.88 \pm 2.54	78.70 \pm 0.59	89.07 \pm 0.11	95.18 \pm 0.28	91.84 \pm 0.09	87.41 \pm 1.74	86.93 \pm 0.15	84.61	5.61
Block	86.59 \pm 1.45	61.18 \pm 1.74	79.78 \pm 2.22	89.08 \pm 0.15	95.45\pm0.19	91.88 \pm 0.05	87.71 \pm 2.95	86.95 \pm 0.08	84.83(+0.22)	5.13
Block+GMoE	87.02 \pm 0.76	62.81 \pm 1.51	79.78 \pm 1.35	89.21 \pm 0.20	95.41 \pm 0.28	92.18 \pm 0.11	89.10 \pm 0.78	87.17\pm0.20	85.34(+0.73)	4.33
Block+EMoE-learn	87.31 \pm 1.23	62.24 \pm 1.51	79.54 \pm 0.17	89.33 \pm 0.11	95.30 \pm 0.09	92.20 \pm 0.09	88.59 \pm 1.68	87.06 \pm 0.18	85.20(+0.59)	4.05
Block+EMoE	87.86 \pm 0.98	62.88\pm0.54	80.05\pm0.29	89.18 \pm 0.25	95.49\pm0.39	92.10 \pm 0.15	89.69 \pm 0.15	86.87 \pm 0.11	85.52(+0.91)	5.71
EMoE	87.75 \pm 0.14	62.27 \pm 0.93	80.02 \pm 0.34	89.37 \pm 0.30	95.41 \pm 0.32	92.10 \pm 0.15	89.58 \pm 0.10	87.06 \pm 0.25	85.45(+0.84)	3.88
EMoE+LN	88.05\pm0.35	63.11\pm0.51	79.90 \pm 1.51	89.40 \pm 0.22	95.18 \pm 0.28	92.23 \pm 0.11	89.70 \pm 0.09	87.03 \pm 0.14	85.58(+0.97)	4.39
EMoE-learn	87.93 \pm 0.61	61.50 \pm 1.09	79.90 \pm 0.61	89.48 \pm 0.24	95.18 \pm 0.11	92.33\pm0.093	89.71\pm0.06	87.00 \pm 0.19	85.38(+0.77)	4.40
EMoE-learn+LN	87.04 \pm 1.11	62.64 \pm 0.84	79.78 \pm 0.59	89.50\pm0.22	95.30 \pm 0.50	92.31 \pm 0.19	89.43 \pm 0.35	87.00 \pm 0.12	85.38(0.77)	3.67

Table 11: ID and OOD results of BERT-L for different settings. "LoRA-to-EMoE" refers to converting a model tuned using standard LoRA into EMoE for testing. On the other hand, "EMoE-to-LoRA" involves merging a tuned EMoE model back into a standard dense model during testing.

Algorithm	CoLA	Gram	MRPC	Twitter	RTE	Hans	SciTail	STSB	Sick	Avg
LoRA	60.89 \pm 2.55	41.77 \pm 1.62	86.83 \pm 0.87	75.42 \pm 2.71	78.70 \pm 1.02	60.37 \pm 1.31	77.36 \pm 0.73	89.22 \pm 0.13	78.48 \pm 0.33	72.12
LoRA-to-EMoE	61.31 \pm 2.14	41.99 \pm 1.56	86.83 \pm 0.91	75.15 \pm 3.02	78.58 \pm 0.95	60.39 \pm 1.32	77.24 \pm 0.68	89.23 \pm 0.13	78.53 \pm 0.35	72.14
EMoE	62.69 \pm 0.91	42.95 \pm 0.95	87.82 \pm 0.17	76.07 \pm 2.12	79.54 \pm 0.45	61.56 \pm 1.65	78.09 \pm 0.56	89.39 \pm 0.31	78.57 \pm 0.67	72.96
EMoE-to-LoRA	62.69 \pm 0.91	42.94 \pm 0.95	87.82 \pm 0.17	76.06 \pm 2.12	79.54 \pm 0.45	61.56 \pm 1.65	78.07 \pm 0.58	89.39 \pm 0.3	78.58 \pm 0.67	72.96

Table 12: ID results of BERT-L for different settings. "Cluster-top" refers to EMoE utilizing avg-k gating. "Cluster-not-top" represents a scenario where, during gating, the top-k experts are removed. Similarly, "Cluster-bottom" involves selecting the bottom-k experts with the lowest scores during gating. "Random" denotes the approach of randomly selecting key values to construct experts. The terms "top," "not-top," and "bottom" have the same meanings as in the cluster situations.

Algorithm	MRPC	CoLA	RTE	STSB	SST2	QNLI	Avg
LoRA	89.97 \pm 0.40	63.40 \pm 0.62	72.92 \pm 1.64	90.51 \pm 0.18	93.16 \pm 0.19	92.20 \pm 0.13	83.69
Cluster-top	90.85\pm0.61	65.33\pm0.40	75.21\pm1.62	90.54 \pm 0.03	93.50 \pm 0.33	92.23 \pm 0.10	84.61(+0.92)
Cluster-not-top	89.61 \pm 0.76	63.21 \pm 0.44	72.56 \pm 1.28	90.31 \pm 0.07	93.12 \pm 0.34	92.14 \pm 0.18	83.49(-0.20)
Cluster-bottom	89.21 \pm 0.69	63.08 \pm 1.09	71.72 \pm 0.34	90.15 \pm 0.18	92.97 \pm 0.19	92.13 \pm 0.31	83.21(-0.48)
Random-top	89.88 \pm 0.75	63.26 \pm 0.39	72.56 \pm 1.06	90.33 \pm 0.05	93.35 \pm 0.00	92.14 \pm 0.20	83.59(-0.11)
Random-not-top	90.09 \pm 0.75	63.35 \pm 0.34	72.44 \pm 1.19	90.44 \pm 0.07	93.31 \pm 0.25	92.20 \pm 0.16	83.64(-0.05)
Random-bottom	89.47 \pm 0.23	63.17 \pm 0.98	71.96 \pm 0.74	90.30 \pm 0.23	93.11 \pm 0.25	92.10 \pm 0.11	83.35(-0.34)

Table 13: Raw OOD performances across 13 tasks. Average results with standard deviation and best results are reported separately. Due to the large deviation across seeds overall methods, we use Friedman rank metrics (Friedman, 1940).

Algorithm	Twitter-M	GrammarTest	Hans	SciTail	Sick-S	NewsQA	Amazon	Flipkart	Indb	Yelp	MRPC	Twitter-Q	Sick-M
BERT-Large (340 Million Parameters) Results (mean and standard deviation)													
LoRA	80.09 \pm 0.49	43.55 \pm 1.34	55.51 \pm 1.94	81.13 \pm 0.88	81.63 \pm 0.16	78.22 \pm 0.17	89.06 \pm 1.81	91.79 \pm 0.27	84.97 \pm 1.32	88.40 \pm 2.06	71.73 \pm 0.46	78.10 \pm 0.33	53.17 \pm 0.92
LoRA+block	80.70 \pm 0.35	42.94 \pm 0.47	54.35 \pm 1.08	80.99 \pm 0.33	81.58 \pm 0.18	78.33 \pm 0.24	88.21 \pm 1.20	91.26 \pm 0.96	84.10 \pm 0.85	89.13 \pm 0.20	71.57 \pm 0.87	79.22 \pm 0.59	53.67 \pm 0.77
GMoE	81.17 \pm 0.54	46.76 \pm 1.91	58.73 \pm 0.74	79.41 \pm 0.10	81.35 \pm 0.34	78.05 \pm 0.28	89.27 \pm 1.38	91.77 \pm 0.07	84.93 \pm 1.09	88.70 \pm 1.77	71.08 \pm 0.69	78.70 \pm 0.37	53.85 \pm 1.27
Block+EMoE+learn	81.09 \pm 0.47	43.29 \pm 1.42	57.55 \pm 1.48	77.72 \pm 0.61	80.78 \pm 0.49	78.32 \pm 0.13	90.17 \pm 0.32	91.82 \pm 0.18	85.71 \pm 0.19	89.62 \pm 0.24	72.71 \pm 0.23	77.85 \pm 1.03	54.69 \pm 0.15
Block+EMoE	81.07 \pm 0.53	46.33 \pm 1.40	53.50 \pm 0.97	79.62 \pm 0.45	80.15 \pm 0.61	79.03 \pm 0.25	88.81 \pm 0.19	91.33 \pm 0.23	84.92 \pm 0.07	88.87 \pm 0.26	70.59 \pm 1.00	74.62 \pm 2.70	53.04 \pm 1.82
EMoE	80.82 \pm 0.10	44.18 \pm 0.63	61.30 \pm 2.24	76.93 \pm 2.52	81.19 \pm 0.27	77.87 \pm 0.19	90.25 \pm 0.10	92.14 \pm 0.25	85.63 \pm 0.30	90.21 \pm 0.14	71.24 \pm 1.22	78.00 \pm 0.87	51.55 \pm 0.88
EMoE+In	81.04 \pm 0.10	45.05 \pm 0.88	58.17 \pm 1.81	77.92 \pm 1.64	81.27 \pm 0.17	77.40 \pm 0.25	90.08 \pm 0.07	91.64 \pm 0.54	85.67 \pm 0.29	89.23 \pm 0.67	72.14 \pm 0.76	77.34 \pm 1.33	52.81 \pm 0.48
EMoE+learn	81.08 \pm 0.24	46.09 \pm 2.12	57.56 \pm 0.43	77.52 \pm 2.15	81.25 \pm 0.13	78.16 \pm 0.30	89.84 \pm 0.13	91.87 \pm 0.28	84.97 \pm 0.33	89.76 \pm 0.33	71.32 \pm 2.03	77.47 \pm 0.76	53.29 \pm 0.45
EMoE+learn+In	81.34 \pm 0.30	44.46 \pm 1.67	58.38 \pm 0.59	77.78 \pm 1.71	81.13 \pm 0.26	78.28 \pm 0.13	90.02 \pm 0.29	91.48 \pm 0.30	85.62 \pm 0.46	89.87 \pm 0.30	71.90 \pm 0.61	77.38 \pm 1.77	53.44 \pm 0.47
BERT-Large (340 Million Parameters) Results (best result)													
LoRA	80.75	45.42	58.24	82.03	81.79	78.46	90.35	92.05	85.95	90.37	72.06	78.41	54.44
LoRA+block	81.19	43.56	55.48	81.45	81.83	78.63	89.49	92.48	85.25	89.17	72.79	79.88	54.71
GMoE	81.78	49.14	59.72	79.55	81.66	78.41	90.31	91.86	85.93	90.42	72.06	79.02	55.16
Block+EMoE+learn	81.72	44.45	61.70	78.47	81.38	78.46	90.59	92.04	85.93	89.95	73.04	78.89	54.91
Block+EMoE	81.49	47.77	54.57	80.15	80.85	79.32	88.98	91.66	85.00	89.23	71.81	77.14	55.56
EMoE	80.95	45.05	64.31	79.64	81.55	78.10	90.37	92.42	86.03	90.34	72.55	79.23	52.24
EMoE+In	81.17	45.71	60.73	79.84	81.48	77.63	90.15	92.33	86.01	90.60	72.79	79.53	53.28
EMoE+learn	81.34	48.75	58.11	79.89	81.25	78.58	89.93	92.23	85.38	90.21	74.02	78.33	53.91
EMoE+learn+In	81.72	46.82	59.09	79.60	81.41	78.47	90.27	91.72	86.11	90.17	72.55	78.67	54.10
GPT2-XL (1.5 Billion Parameters) Results (mean and standard deviation)													
LoRA	75.42 \pm 2.71	41.78 \pm 1.62	60.37 \pm 1.32	77.36 \pm 0.73	78.48 \pm 0.33	78.57 \pm 0.59	89.91 \pm 0.73	90.05 \pm 0.44	85.57 \pm 1.34	88.85 \pm 0.38	68.22 \pm 1.27	73.60 \pm 2.87	57.39 \pm 0.34
LoRA+block	76.87 \pm 2.47	41.09 \pm 1.80	58.67 \pm 0.97	78.57 \pm 1.23	77.66 \pm 0.25	78.78 \pm 0.55	90.11 \pm 0.71	91.54 \pm 0.94	83.54 \pm 0.57	88.85 \pm 1.01	69.53 \pm 0.64	68.22 \pm 7.84	58.53 \pm 0.46
GMoE	75.28 \pm 3.67	42.50 \pm 1.37	62.59 \pm 0.37	77.89 \pm 0.56	78.33 \pm 0.58	79.18 \pm 0.04	90.11 \pm 0.38	88.64 \pm 4.52	83.23 \pm 0.40	89.47 \pm 0.26	70.10 \pm 1.39	74.61 \pm 3.71	58.29 \pm 0.78
Block+EMoE+learn	74.80 \pm 5.15	44.11 \pm 1.95	61.67 \pm 1.18	78.18 \pm 0.04	78.27 \pm 0.21	78.97 \pm 0.20	90.22 \pm 0.59	91.04 \pm 0.65	83.82 \pm 0.54	69.93 \pm 0.67	73.41 \pm 3.94	57.58 \pm 0.57	57.34 \pm 3.94
Block+EMoE	75.37 \pm 4.04	39.33 \pm 2.21	58.32 \pm 2.40	72.05 \pm 3.04	77.70 \pm 0.59	79.32 \pm 0.06	90.22 \pm 0.59	91.79 \pm 0.27	83.79 \pm 0.27	89.23 \pm 0.38	63.24 \pm 8.56	70.60 \pm 2.89	56.83 \pm 0.57
EMoE	76.07 \pm 2.12	42.95 \pm 0.95	61.56 \pm 1.65	78.09 \pm 0.56	78.57 \pm 0.67	78.87 \pm 0.38	90.39 \pm 0.55	91.87 \pm 0.22	83.55 \pm 1.04	89.14 \pm 1.39	67.73 \pm 1.55	74.06 \pm 4.79	57.33 \pm 0.59
EMoE+In	74.35 \pm 3.50	42.24 \pm 0.89	61.88 \pm 2.45	78.32 \pm 0.95	78.67 \pm 0.62	79.02 \pm 0.30	89.51 \pm 0.90	91.19 \pm 0.56	83.12 \pm 1.90	89.29 \pm 1.09	69.20 \pm 1.03	72.74 \pm 5.10	57.62 \pm 0.02
EMoE+learn	74.61 \pm 4.75	40.50 \pm 0.46	59.50 \pm 3.74	80.04 \pm 0.46	78.27 \pm 0.59	79.06 \pm 0.30	90.59 \pm 0.66	91.69 \pm 0.59	83.23 \pm 1.54	89.79 \pm 1.35	67.48 \pm 1.30	73.62 \pm 1.12	56.22 \pm 0.15
EMoE+learn+In	77.17 \pm 1.58	42.52 \pm 0.41	58.90 \pm 4.16	79.56 \pm 0.81	78.27 \pm 0.54	79.19 \pm 0.32	90.23 \pm 0.86	91.98 \pm 0.35	83.31 \pm 1.08	88.50 \pm 1.92	68.63 \pm 1.51	71.26 \pm 3.49	56.69 \pm 0.37
GPT2-XL (1.5 Billion Parameters) Results (best result)													
LoRA	78.17	43.93	61.77	78.39	78.87	79.12	90.52	91.03	84.81	89.39	69.12	77.48	57.79
LoRA+block	80.17	43.09	59.52	79.45	78.33	79.42	90.94	92.87	84.12	90.28	70.10	74.55	57.64
GMoE	80.23	43.96	63.05	78.68	78.00	79.33	90.57	92.27	83.69	89.81	71.08	79.79	59.36
Block+EMoE+learn	80.04	46.01	62.74	79.06	79.24	80.67	91.94	84.45	90.42	70.59	78.78	58.28	
Block+EMoE	79.02	41.55	61.64	76.30	78.33	79.40	90.68	92.00	84.12	89.60	73.31	73.31	57.64
EMoE	77.58	43.84	63.78	78.75	79.29	79.26	91.17	92.19	84.42	90.22	69.85	80.81	58.01
EMoE+In	77.92	43.39	65.32	79.16	79.35	90.48	91.74	85.73	90.79	70.59	79.81	57.87	
EMoE+learn	79.35	41.15	64.56	80.40	78.76	79.76	91.32	92.47	84.49	90.77	69.12	74.77	56.42
EMoE+learn+In	79.35	43.01	64.32	80.57	79.02	79.63	91.40	92.41	84.84	90.57	70.34	74.77	57.13

Table 14: Results of different MoEs Configurations

Algorithm	MRPC	CoLA	RTE	STSB	Avg
Dense	86.83 \pm 0.87	60.88 \pm 2.54	78.70 \pm 0.59	89.07 \pm 0.11	78.87
EMoE	88.05 \pm 0.35	63.11 \pm 0.21	80.02 \pm 0.34	89.37 \pm 0.24	80.14
EMoE-learn	87.93 \pm 0.61	62.87 \pm 0.71	79.90 \pm 0.61	89.40 \pm 0.08	80.03
EMoE-last-every2	87.27 \pm 0.47	61.60 \pm 0.63	79.18 \pm 0.17	89.38 \pm 0.24	79.36
EMoE-learn-learn-every2	87.26 \pm 0.21	61.82 \pm 1.10	78.46 \pm 1.22	89.31 \pm 0.15	79.21
EMoE-every2	86.78 \pm 0.34	59.21 \pm 0.79	77.38 \pm 1.04	89.31 \pm 0.06	78.17
EMoE-learn-every2	86.71 \pm 1.32	54.02 \pm 0.47	74.25 \pm 0.74	88.51 \pm 0.31	75.87

Table 15: Comparison of EMoE and Dense Results with Different Training Data Fraction

Data Fraction	CoLA		MRPC		RTE		STSB		SST2		QNLI		Average Diff
	EMoE	Dense											
1.0	62.27	60.88	87.75	86.83	80.02	78.70	89.37	89.07	95.41	95.18	92.10	91.84	0.74
0.9	61.58	60.01	87.52	86.49	79.87	77.85	89.18	89.07	95.41	95.16	92.05	91.94	0.85
0.8	60.89	59.28	86.58	86.35	79.22	76.77	88.98	88.99	95.34	95.06	91.94	91.83	0.78
0.7	59.29	58.25	86.10	85.56	77.98	76.77	87.95	87.95	95.41	95.06	92.04	91.74	0.57
0.6	58.91	57.93	85.61	84.76	76.29	75.45	86.70	86.17	95.26	95.03	91.83	91.54	0.62
0.5	55.18	53.89	84.91	84.76	76.53	75.21	85.63	85.59	95.19	94.91	91.23	91.12	0.53
0.3	50.17	50.29	82.80	82.59	73.52	72.44	80.23	79.08	94.82	94.72	90.45	90.26	0.44
0.1	46.47	45.54	78.17	77.85	63.05	63.17	62.33	60.81	94.49	94.38	88.39	88.32	0.47

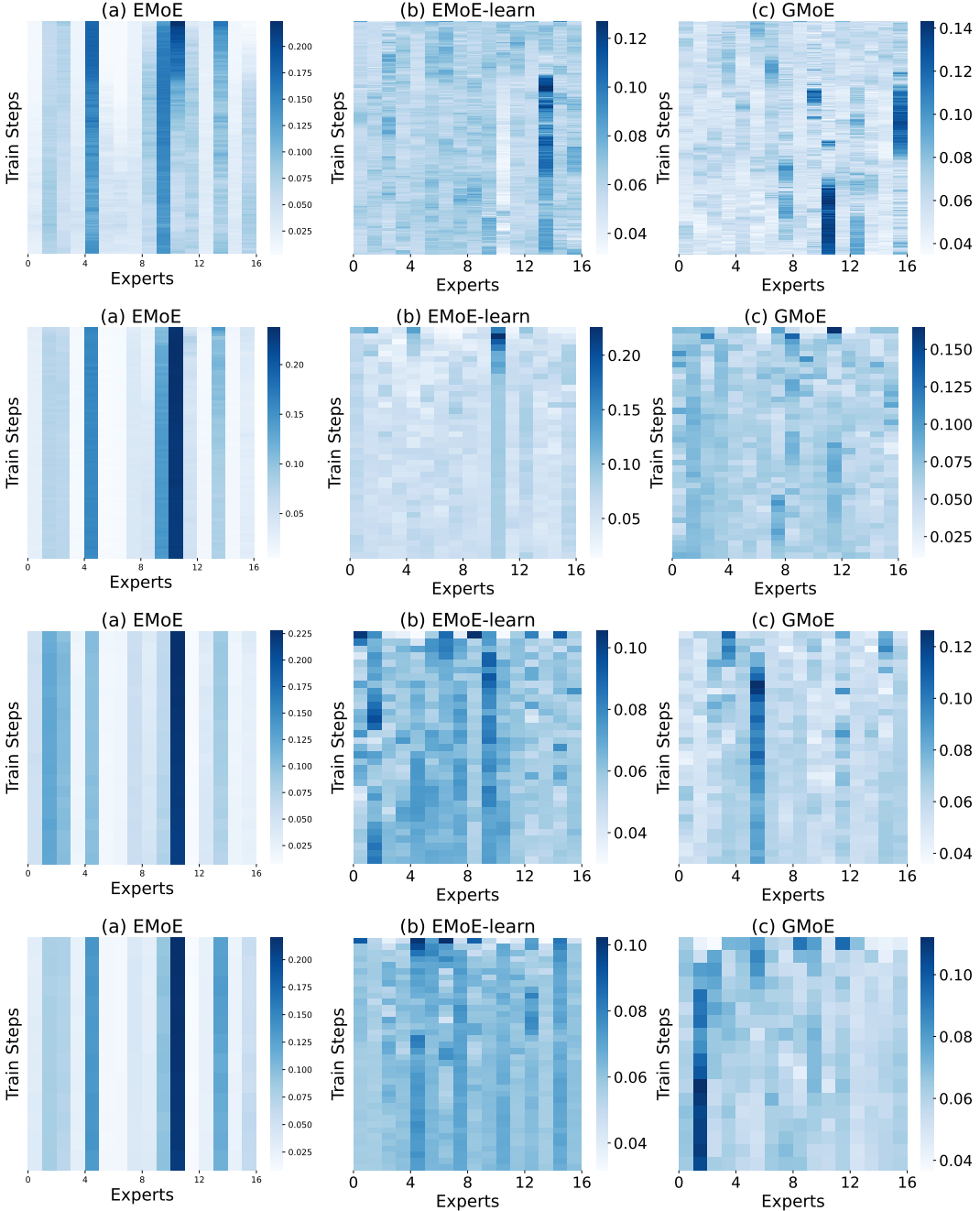


Figure 8: Expert selections during training with distinct gating functions (avg-k vs learned gate) and expert types (modules from dense vs repetitions of dense). The vertical axis illustrates training steps, with top-down arrangement signifying begin-end; the horizontal axis represents expert selection frequency within 1K steps. (a), (b) and (c) correspond respectively to EMoE, EMoE-learn, and GMoE configurations. The subplots from top to bottom are results for SST-2, STS-B, MRPC, and RTE.